Limit State Response of Composite Columns and Beam-Columns Part II: Application of Design Provisions for the 2005 AISC Specification

ROBERTO T. LEON and JEROME F. HAJJAR

The strength of composite beam-columns, including steel sections encased in concrete (also known as SRC) and steel sections filled with concrete (CFT), as presented in the 2005 AISC *Specification for Structural Steel Buildings*, ANSI/AISC 360-05 (AISC, 2005a), hereafter referred to as the 2005 AISC *Specification*, must be computed based on first principles of mechanics and reasonable models for the stress-strain characteristics of the materials. Chapter I of the 2005 AISC *Specification* provides two options to fulfill this requirement: a general approach labeled the strain-compatibility method and a simplified approach labeled the plastic stress distribution method.

The strain-compatibility method is conceptually similar to conducting cross section analysis of a reinforced concrete section, and requires the designer to:

1. Subdivide the cross section into a large number of areas (termed "fibers");
2. Assume a strain distribution across the cross-section and a location of the neutral axis;
3. Compute stresses based on the assumed stress-strain relationships for the different components (unconfined and confined concrete, reinforcing bars, and the steel shape);
4. Integrate the stresses over the cross section to obtain the total axial load and the moment about the plastic neutral axis (or other commonly assumed axis);
5. Iterate steps 2 through 4 to obtain an axial load-moment interaction surface for the column.

Roberto T. Leon is professor, school of civil and environmental engineering, Georgia Tech, Atlanta, GA and former chair, AISC Task Committee 5 on Composite Construction.

Jerome F. Hajjar is professor, department of civil and environmental engineering, University of Illinois, Urbana, IL.

The designer is free to use any reasonable assumptions, including a nonlinear strain distribution in step 2 and nonlinear material properties in step 3, so long as those assumptions are supported by analyses, test data, or other documentation. In general, the analysis is run with an assumption of a linear strain distribution in step 2 and simplified uniaxial material relationships in step 3.

Figure 1 illustrates the strain-compatibility procedure. Figure 1a shows the subdivision of the cross-section into a series of square "fibers" representing four different materials: unconfined concrete outside the ties, confined concrete inside the ties (shaded), reinforcing bar steel, and rolled shape steel. Figure 1b shows a linear strain distribution with an arbitrary location of the neutral axis. Figure 1c shows the material properties. For each material, it shows both the nonlinear stress-strain curves as may be assumed for the strain-compatibility analysis and the bilinear rigid-plastic curves (dashed lines) that would be assumed for a simplified analysis; for example, a plastic strength calculation. Figure 1d shows the stress distributions for the situation usually used to compute the ultimate strength of the cross-section, in other words, when the strain in the concrete, ε_c, has reached 0.003 and the steel strain in the extreme fiber of the steel shape, ε_s, has exceeded its yield strain. The concrete stress blocks are shown separately for clarity. Note that for this case the unconfined stress-strain relationship is shown up to the top edge of the section. Figure 1e shows a stress distribution when the concrete strain has exceeded 0.003 and the steel shape and reinforcing bars are well into the strain-hardening range. In this case the confined concrete stress-strain relationship is used, but limited to the confined section; the unconfined section has spalled off. Figure 1f shows the typical stress distribution used for the plastic stress distribution case. Note that this stress distribution does not correspond exactly to any "real" stress distribution but is considered as a conservative approximation for a section that can sustain concrete strain on the order of 0.005 and steel strains larger than 0.01.

In Figure 2, three qualitative curves are shown for the stress distributions shown in Figures 1d through f. The first curve is for the strength envelope consistent with a concrete strain of 0.003 at the extreme fiber (Figure 1d) while the

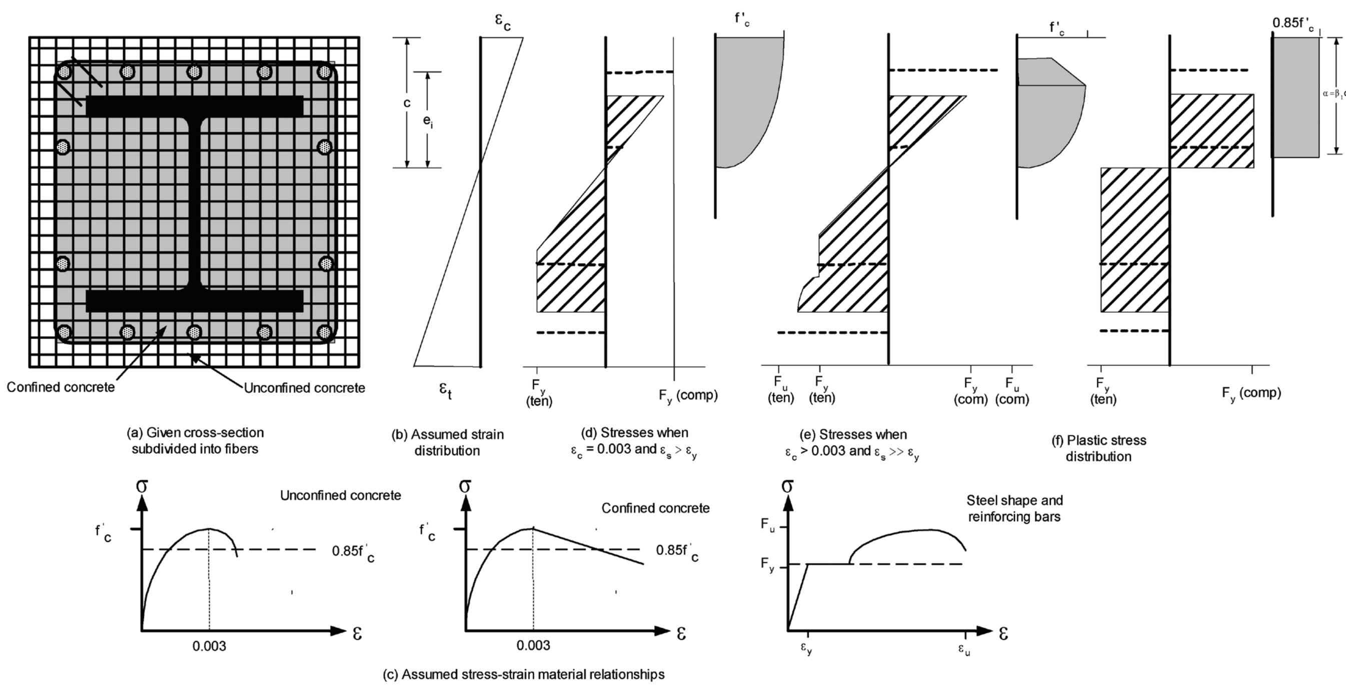

Fig. 1. Development of composite beam-column cross-section strength.

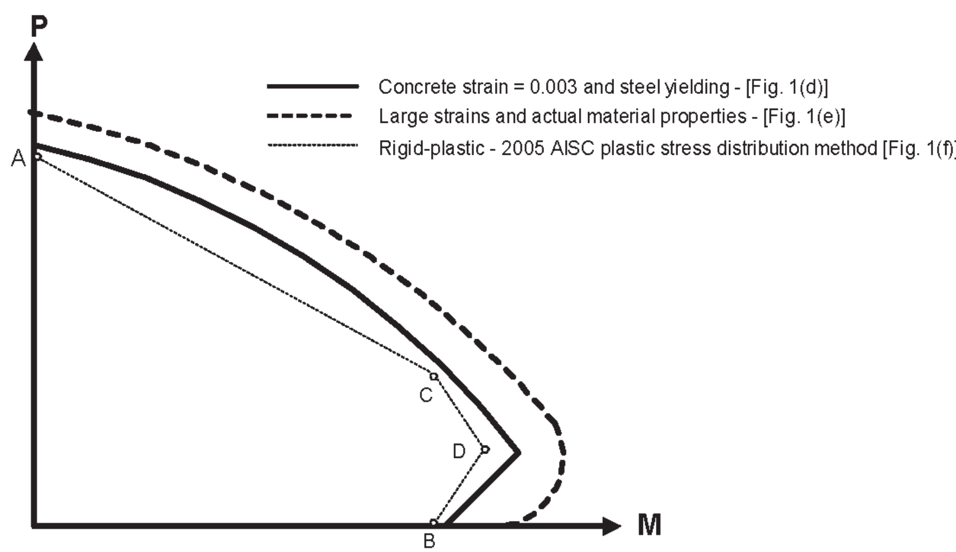

Fig. 2. Interaction diagrams based on the stress distributions shown in Figure 1d through 1f.

second curve is for a concrete strain of approximately 0.005 at the same location (Figure 1e). In the latter case, the effect of the unconfined concrete has been eliminated and only the confined concrete core is contributing. Figure 2 also shows the corresponding strength envelope assuming bilinear rigid-plastic stress-strain curves for the materials and calculated only for the position of the neutral axis at four discrete points (Figure 1f) rather than continuously. The latter corresponds to the simplified approach (plastic stress distribution method) used in the 2005 AISC *Specification*.

It should be noted that the strain-compatibility method discussed here is the only one currently applicable to cases with biaxial loading if one wants to generate interaction points in addition to the anchor points on the coordinate axes of the interaction diagram. For that case the procedure is analogous to that described in Figure 1, except that the section will not be aligned along its principal axes as currently shown in Figure 1a but at some other angle. The calculations will become more laborious and there are only approximate solutions available for the case of CFT columns, which can be treated as reinforced concrete columns with distributed reinforcement and distance between extreme bar layers equal to the section depth. However, the use of the interaction equations of AISC 2005 *Specification* Chapter H (AISC, 2005a), discussed below, provides an alternative procedure in which only the anchor points on the coordinate axes of the interaction diagram need to be computed.

The procedure discussed here is meant for monotonic loading cases; for seismic design further attention to confinement and local buckling phenomena will be needed to sustain the strength envelopes shown in Figure 2 under large cyclic deformations. The strain compatibility method is now embedded in a number of commercial structural analysis and design software packages for reinforced concrete sections and is accessible to most engineers. Thus the 2005 AISC *Specification* explicitly endorses the use of these advanced design tools. However, this approach is time-consuming and not always useful for preliminary design.

The plastic stress distribution method proposed in Chapter I of the 2005 AISC *Specification* is based on the plastic stress distributions shown by the dashed lines in the material properties in Figure 1. This method is intended to provide a design-oriented approach that captures the essential features of the strain compatibility one, but without the associated complexities (Roik and Bergmann, 1992). This approach is described in detail in this paper, which begins with a discussion of the axial compressive strength of different composite cross sections and then moves on to the design of composite beam-columns. The materials are assumed to be elasto-plastic, with no attempt to include deformation capacity (ductility) in the calculations. The assumption is that the confinement required by the AISC *Specification* for encased shapes and that provided by the tubes in CFTs is sufficient to provide the limited ductility required for the steel to yield significantly ($\varepsilon_s > 0.005$) while the concrete compressive strength has not decreased below that given by an assumption of a uniform stress of $0.85f'_c$ for SRCs and rectangular CFTs ($0.95f'_c$ for circular CFTs) over an effective depth similar to that used in conventional reinforced concrete design. These assumptions are well within those made in Section 10.2 and 10.3 of the ACI Code (ACI, 2005), and thus this approach is deemed to satisfy both the current steel and concrete design specifications. Note that the AISC *Steel Construction Manual* (AISC, 2005b) indicates that the 0.95 factor for circular CFTs is for the uniform compression case only. However, the calibrations were conducted assuming 0.95 for any interaction condition and thus that value is used in this paper for all calculations for circular CFTs (Kim, 2005). The confinement resulting from hoop stresses in circular tubes could justify a larger factor in many practical cases, but other checks on the column slenderness and the eccentricity of the load would be required. The 0.95 factor was selected as a reasonable lower bound value that would not require such further checks.

The simplified or plastic stress distribution method is analogous to the strain-compatibility method used to determine the strength of a reinforced concrete column, but rather than solving for a large number of points along the interaction diagram, it relies on linear interpolation between four points for major axis bending for encased composite sections or five points for minor axis bending of encased composite sections and all filled composite sections (Figure 3). Aside from these anchor points, the remaining points are approximations to the exact interaction curve. Designers can use the strain-compatibility method to check the plastic stress distribution method, but similar results will only be obtained if the assumed stress-strain curves for the strain compatibility method are the same as those for the plastic method.

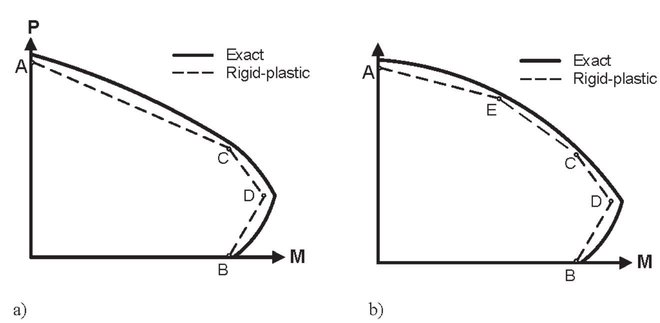

Fig. 3. Interaction diagrams for composite beam-columns: a) encased composite sections, strong axis, and filled composite sections; and b) encased composite sections, weak axis.

PRELIMINARY SIZING OF COMPOSITE SECTIONS FOR AXIAL COMPRESSION

For systems in which the composite columns are assumed to carry primarily gravity loads, or for in assessing composite beam-column strength, the design process outlined below as per the plastic stress distribution method may be used to compute the design axial compressive strength. This may be used with the required strength, P_u, to assess the axial strength of the member.[1] See Leon, Kim and Hajjar (2007) for a summary of all design equations discussed in this procedure.

1. Select the steel shape and reinforcing bars yield strengths, F_y and F_{yr}, respectively, and the concrete compressive strength, f_c'.

2. Select a steel ratio, ρ, for the column. This ratio refers to the area of the steel shape only, A_s, to the gross area of concrete, A_g. The influence of the rebar will be ignored in this design procedure because the AISC *Specification* does not consider them in the calculations of the steel area. For encased composite sections in gravity systems, reasonable and economic sizes result from assuming ρ is in the range of 8 to 12%. For filled composite sections, the range for ρ is typically 6 to 10%.

3. Select a slenderness ratio for the column. Most composite columns are not very slender, so the reduction in the nominal axial strength due to length effects is often smaller than that for regular steel columns of the same length. Most composite columns in gravity frames will have a slenderness parameter $\lambda = \sqrt{P_o/P_e}$ between 0.5 and 1.0 (corresponding to reductions for length effects of 80 to 65%). This reduction value will be termed β and a value of 0.7 is recommended for initial trial designs.

4. Calculate the required gross area of the concrete based on Equation I2-4 from ANSI/AISC 360-05 (AISC, 2005a) [termed in this paper Equation (AISC 2005 I2-4)]:

$$\frac{P_o}{\phi_c \beta} = A_s F_y + A_{sr} F_{yr} + 0.85 A_c f_c', \text{ kips (kN)} \quad \text{(AISC 2005 I2-4)}$$

   In the design of SRCs, one can assume that for this calculation $A_s \approx \rho A_g$, $A_{sr} \approx 0.3\rho A_g$ and $A_c = (1 - 1.3\rho)A_g$. For circular concrete-filled steel tubes (CCFT), assume $A_s \approx \rho A_g$, $A_{sr} = 0$, and $A_c = (1 - \rho)A_g$. For CCFTs, 0.95 may be used in the last term instead of 0.85 to account for the effects of confinement [see Equation (AISC 2005 I2-13)]. For encased sections and rectangular concrete-filled tubes (RCFTs), an approximation of Equations (AISC 2005 I2-4) and (AISC 2005 I2-13) can be used to find the preliminary size of the column as follows (and a similar formula is shown for circular concrete-filled tubes):

$$A_g \approx \frac{P_o}{\phi\, \beta \left[\rho F_y + 0.3\rho F_{yr} + 0.85 f_c' (1 - 1.3\rho) \right]} \quad \text{(SRC and RCFT)}$$

$$A_g \approx \frac{P_o}{\phi_c \beta \left[\rho F_y + 0.95 f_c' \ (1 - \rho) \right]} \quad \text{(CCFT)}$$

5. Assume a preliminary section size and reinforcement based on A_g calculated above and begin the checking procedure. For filled composite sections, first check local buckling of the steel tube as per AISC (2005a).

6. Determine the coefficient C_1 or C_3 from Equation (AISC 2005 I2-7) for encased composite sections or Equation (AISC 2005 I2-15) for filled composite sections:

$$C_1 = 0.1 + 2\left(\frac{A_s}{A_c + A_s}\right) \quad \text{(AISC 2005 I2-7)}$$

$$\approx (0.1 + 2\rho) \le 0.3$$

$$C_3 = 0.6 + 2\left(\frac{A_s}{A_c + A_s}\right) \quad \text{(AISC 2005 I2-15)}$$

$$\approx (0.6 + 2\rho) \le 0.9$$

7. Compute the equivalent stiffness (EI_{eff}) from Equation (AISC 2005 I2-6) for encased composite sections or (AISC 2005 I2-14) for filled composite sections:

$$EI_{eff} = E_s I_s + 0.5 E_s I_{sr} + C_1 E_c I_c, \text{ kip-in.}^2 \text{ (N-mm}^2) \quad \text{(AISC 2005 I2-6)}$$

$$EI_{eff} = E_s I_s + 1.0 E_s I_{sr} + C_3 E_c I_c, \text{ kip-in.}^2 \text{ (N-mm}^2) \quad \text{(AISC 2005 I2-14)}$$

[1] For a complete set of notations, see Appendix A.

8. Compute the elastic Euler buckling load, P_e, from Equation (AISC 2005 I2-5) for buckling about the axis that provides the lower buckling strength:

$$P_e = \pi^2(EI_{eff}) / (KL)^2, \text{ kips (kN)} \qquad \text{(AISC 2005 I2-5)}$$

9. Calculate the squash load for the columns from Equation (AISC 2005 I2-4) or (AISC 2005 I2-13), where C_2 is 0.85 for rectangular tubes and 0.95 for circular pipes:

$$P_o = A_sF_y + A_{sr}F_{yr} + 0.85A_cf_c', \text{ kips (kN)} \qquad \text{(AISC 2005 I2-4)}$$

$$P_o = A_sF_y + A_{sr}F_{yr} + C_2A_cf_c', \text{ kips (kN)} \qquad \text{(AISC 2005 I2-13)}$$

This load corresponds to the stress distribution shown in Part (a) of Table 1, or Point A in Tables 2 through 5. This is the maximum axial compressive load that the cross-section can carry if strain-hardening of the steel and additional strength due to the confinement of the concrete are ignored.

10. For design, this maximum strength needs to be adjusted to account for length effects through either Equation (AISC 2005 I2-2) or (AISC 2005 I2-3). This adjustment is based on the ratio of P_o/P_e for the governing axis of buckling; this ratio corresponds to the slenderness ratio, λ_c^2, used in previous versions of the AISC *Specification*:

(a) When $P_e \geq 0.44P_o$:

$$P_n = P_o\left[0.658^{\left(\frac{P_o}{P_e}\right)}\right], \text{ kips (kN)} \qquad \text{(AISC 2005 I2-2)}$$

(b) When $P_e < 0.44P_o$:

$$P_n = 0.877P_e, \text{ kips (kN)} \qquad \text{(AISC 2005 I2-3)}$$

11. For design, the value of P_n is then adjusted by the appropriate resistance factor, ϕ_c, or safety factor, Ω_c, for LRFD or ASD:

$$\phi_c = 0.75 \text{ (LRFD)} \quad \Omega_c = 2.00 \text{ (ASD)}$$

Design Examples

Example 1: Encased Concrete Column (SRC)

Design an encased composite column to resist a required axial strength of 4,000 kips (LRFD) with a KL = 24 ft. Use F_y = 50 ksi, F_{yr} = 60 ksi and f_c' = 8 ksi. Assume the column is continuously braced about the minor axis. In Examples 1 through 3, all the material and similar limitations in AISC Sections I1.2, I2.1a and I2.2a are satisfied. Checking of those limits will be illustrated in Example 4.

1. Select an initial steel ratio, ρ, of 10% for the column.

2. Assume $\beta = 0.7$.

3. Calculate the required gross area:

$$A_g \approx \frac{P_o}{\phi_c\beta\left[\rho F_y + 0.3\rho F_{yr} + 0.85f_c'(1-1.3\rho)\right]}$$

$$= \frac{4{,}000}{(0.75)(0.7)\left[(0.1)(50) + 0.3(0.1)(60) + (0.85)(8)(0.87)\right]}$$

$$A_g \approx 599 \text{ in.}^2$$

4. Assuming a square column, this gross area will roughly require a 24 in. × 24 in. column. The steel section will require an $A_s \approx 59.9$ in.^{2} to achieve the desired steel ratio. Select a W14×211 (A_s = 62.0 in.^{2}) buckling about its major axis and assume 16-#8 bars distributed along the perimeter of the section providing a rebar reinforcement ratio of approximately 2.2% (see Figure 4). Many of these reinforcing bars will be needed to maintain confinement and rebar spacing requirements, and will not

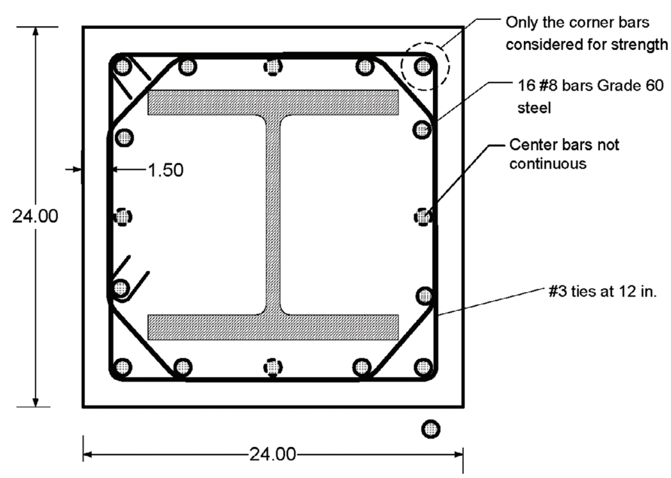

Fig. 4. SSRC section for Example 1.

necessarily be continuous through the joint due to the presence of framing beams. In this example, only the four corner bars, located at a distance of 9.63 in. from the column centerline, will be assumed as continuous and used in the strength calculations [A_{sr} = 4(0.79 in.^{2})]. For this section:

A_s = 62.0 in.^{2}
$I_s = I_x$ = 2,660 in.^{4}
Z_x = 390 in.^{3}
A_{sr} = 3.16 in.^{2}
$A_c = A_g - A_s - A_{sr}$ = (24)(24) – 62.0 – 3.16 = 511 in.^{2}
e_1 = 9.63 in. (distance from the column centerline to reinforcing bars)
$I_{sr} \approx (A_{sr})(e_1)^2$ = 293 in.^{4}
w_c = 148.1 lb/ft^3, assumed

$$E_c = w_c^{1.5}\sqrt{f_c'}\ \text{(ksi)}\ \text{(AISC)} = 57{,}000\sqrt{f_c'(\text{psi})}\ \text{(ACI)}$$

$$E_c = (148.1\ \text{lb/ft}^3)^{1.5}\sqrt{8\ \text{ksi}} = 5{,}100\ \text{ksi}$$

Assume #3 ties at 12 in.

ρ_{st} = 0.22 in.^{2}/12 in. = 0.0183 in.^{2}/in. > 0.009 in.^{2}/in. (ANSI/AISC 360-05, Sect. I2.1a)

5. Determine the coefficient C_1 from Equation (AISC 2005 I2-7):

$$C_1 = 0.1 + 2\left(\frac{A_s}{A_c + A_s}\right) = 0.1 + 2\left(\frac{62.0}{511 + 62.0}\right)$$

$$= 0.316 \text{ but } C_1 \le 0.3 \text{ so } C_1 = 0.3$$

6. Compute the equivalent stiffness, EI_{eff}, from Equation (AISC 2005 I2-6) for encased shapes:

$$EI_{eff} = E_s I_s + 0.5 E_s I_{sr} + C_1 E_c I_c$$

$$EI_{eff} = (29{,}000)(2{,}660) + (0.5)(29{,}000)(293) + (0.316)(5{,}100)\left(\frac{24^4}{12} - 2{,}660 - 293\right)$$

$$EI_{eff} = 121\times10^6\ \text{kip-in.}^2$$

7. Compute the elastic Euler buckling load, P_e, from Equation (AISC 2005 I2-5):

$$P_e = \frac{\pi^2 EI_{eff}}{(KL)^2} = \frac{\pi^2\left(121\times10^6\right)}{\left[(24)(12)\right]^2} = 14{,}400\ \text{kips}$$

8. Calculate the squash load for the column from Equation (AISC 2005 I2-4):

$$P_o = A_s F_y + A_{sr} F_{yr} + 0.85 A_c f_c'$$
$$= (62.0)(50) + (3.16)(60) + (0.85)(511)(8)$$
$$= 6{,}760\ \text{kips}$$

9. Adjust for length effects:

$$\frac{P_e}{P_o} = \frac{14{,}400}{6{,}760}$$
$$= 2.13 > 0.44,\ \text{use ANSI/AISC 360-05 Equation I2-2}$$

$$\frac{P_o}{P_e} = \frac{6{,}760}{14{,}400} = 0.469$$

$$P_n = P_o(0.658)^{\frac{P_o}{P_e}} = 6{,}760(0.658)^{0.469}$$
$$= 5{,}560\ \text{kips}$$

10. Finally, for design, the value of P_n is adjusted as:

$\phi_c P_n$ = (0.75) (5,560)

= 4,170 kips (LRFD) > 4,000 kips **o.k.**

The associated ASD strength is:

P_n/Ω_c = (5,560 kips/2.00) = 2780 kips (ASD)

This should be compared to the required strength based on ASD load combinations.

The final design is shown in Figure 4.

Example 2: Circular Filled Concrete Column (CCFT)

Design a concrete-filled steel tube column to carry a factored axial load of 1,500 kips (LRFD) with an effective length KL = 18 ft. Use F_y = 42 ksi, F_{yr} = 60 ksi and f_c' = 5 ksi.

1. Select a steel ratio, ρ, of approximately 8% for the column.

2. Assume β = 0.7.

3. Calculate the required gross area:

$$A_g \approx \frac{P_o}{\phi_c \beta\left[\rho F_y + 0.95 f_c'(1-\rho)\right]}$$

$$= \frac{1{,}500}{(0.75)(0.7)\left[(0.08)(42) + 0.95(5)(0.92)\right]}$$

$$A_g \approx 370\ \text{in.}^2 = \frac{\pi D^2}{4} \Rightarrow D = 21.7\ \text{in.}$$

4. The computed D exceeds the largest diameter available for circular hollow sections of 20 in. Assuming the same ρ and D = 20 in., the required steel area is $A_s \approx 25.1$ in.² This is about halfway between the areas for a HSS 20.00 × 0.500 and a HSS 20.00 × 0.375. Select the HSS 20.00 × 0.375 and check. For this section:

   $A_s = 21.5$ in.²
   $I_s = I_x = 1{,}040$ in.⁴
   $Z_x = 135$ in.³
   $t = 0.93(0.375) = 0.349$ in. = HSS design thickness
   $A_c = \pi[20 - 2(0.349)]^2/4 = 293$ in.²
   $E_c = (148.1\text{ lb/ft}^3)^{1.5}\sqrt{5\text{ ksi}} = 4{,}030$ ksi

$$\frac{D}{t} = \frac{20}{0.349}$$

$$= 57.3 < 0.15\left(\frac{E}{F_y}\right) = 0.15\left(\frac{29{,}000}{42}\right) = 104 \textbf{ o.k.}$$

5. Determine the coefficient C_3 from Equation (AISC 2005 I2-15) for filled tubes:

$$C_3 = 0.6 + 2\left(\frac{A_s}{A_c + A_s}\right) = 0.6 + 2\left(\frac{21.5}{293 + 21.5}\right)$$

$$= 0.737 \le 0.9 \text{ so } C_3 = 0.737$$

6. Compute the equivalent stiffness, EI_{eff}, from Equation (AISC 2005 I2-14) for concrete-filled tubes:

$$EI_{eff} = E_s I_s + C_3 E_c I_c$$

$$EI_{eff} = (29{,}000)(1{,}040) + (0.737)(4{,}030)\left(\frac{\pi\left[20 - 2(0.349)\right]^4}{64}\right)$$

$$EI_{eff} = 50.4 \times 10^6 \text{ kip-in.}^2$$

7. Compute the elastic Euler buckling load, P_e, from Equation (AISC 2005 I2-5):

$$P_e = \frac{\pi^2 EI_{eff}}{(KL)^2} = \frac{\pi^2(50.4 \times 10^6)}{(18 \times 12)^2} = 10{,}700 \text{ kips}$$

8. Calculate the squash load for the column from Equation (AISC 2005 I2-4):

$$P_o = A_s F_y + 0.95 A_c f_c' = (21.5)(42) + (0.95)(293)(5)$$

$$P_o = 2{,}290 \text{ kips}$$

9. Adjust for length effects:

$$\frac{P_e}{P_o} = \frac{10{,}700}{2{,}290}$$

$$= 4.67 > 0.44 \text{ use ANSI/AISC 360-05 Equation I2-2}$$

$$\frac{P_o}{P_e} = \frac{2{,}290}{10{,}700} = 0.214$$

$$P_n = P_o(0.658)^{\frac{P_o}{P_e}} = 2{,}290(0.658)^{0.214} = 2{,}090 \text{ kips}$$

10. Finally, for design, the value of P_n is adjusted as:

$$\phi_c P_n = (0.75)(2{,}090)$$

$$= 1{,}570 \text{ kips (LRFD)} > 1{,}500 \text{ kips } \textbf{o.k.}$$

   The associated ASD strength is:

   P_n/Ω_c = (2,090 kips/2.00) = 1,050 kips (ASD)

   This should be compared to the required strength based on ASD load combinations.

In the 3rd Ed. AISC *LRFD Manual of Steel Construction* (AISC, 2001), based on the 1999 AISC *LRFD Specification for Structural Steel Buildings*, the tabulated design strength for this section was 1,680 kips; or a difference of –6.5% in strength for the 2005 AISC *Specification* over the 1999 provisions. If the effective length of the column is 40 ft, the ratio of P_o/P_e is 1.06, P_n = 1,470 kips, and ϕP_n = 1,100 kips based on the 2005 AISC *Specification*. The value of ϕP_n = 1220 kips in the 3rd Ed. AISC *LRFD Manual of Steel Construction*, or a difference of –9.8%.

To check the values given for circular columns in the current AISC *Manual* (AISC, 2005b), consider the design of a HSS 18.000 × 0.500 pipe column filled with 4 ksi concrete and an effective length of 24 ft. Repeating the steps above, the key values are:

1. Compute C_3:

$$C_3 = 0.6 + 2\left(\frac{A_s}{A_c + A_s}\right) = 0.6 + 2\left(\frac{25.6}{229 + 25.6}\right)$$

$$= 0.801 \le 0.9 \text{ so } C_3 = 0.801$$

2. Compute the equivalent stiffness, EI_{eff}, from Equation (AISC 2005 I2-14), with $I_{sr} = 0$, for concrete-filled tubes:

$$EI_{eff} = E_s I_s + C_3 E_c I_c$$

$$E_c = (145\text{ lb/ft}^3)^{1.5}\sqrt{4\text{ ksi}} = 3{,}490$$

$$EI_{eff} = (29{,}000)(985) + (0.801)(3{,}490)\left(\frac{\pi\left[18 - 2(0.465)\right]^4}{64}\right)$$

$$EI_{eff} = 40.2 \times 10^6 \text{ kip-in.}^2$$

3. Compute the elastic Euler buckling load, P_e, from Equation (AISC 2005 I2-5):

$$P_e = \frac{\pi^2 EI_{eff}}{(KL)^2} = \frac{\pi^2(40.2\times10^2)}{(24\times12)^2} = 4{,}780 \text{ kips}$$

4. Calculate the squash load for the column from Equation (AISC 2005 I2-13), with $A_{sr} = 0$ and $A_c = \pi[18 - 2(0.465)]^2/4 = 229$ in.^{2}

$$P_o = A_s F_y + 0.95 A_c f_c' = (25.6)(42) + (0.95)(229)(4)$$

$$P_o = 1{,}950 \text{ kips}$$

5. Adjust for length effects:

$$\frac{P_e}{P_o} = \frac{4{,}780}{1{,}950} = 2.45 > 0.44 \text{ use Equation I2-2}$$

$$\frac{P_o}{P_e} = \frac{1{,}950}{4{,}780} = 0.408$$

$$P_n = P_o(0.658)^{\frac{P_o}{P_e}} = 1{,}950(0.658)^{0.408} = 1{,}640 \text{ kips}$$

$\phi_c P_n = (0.75)\,(1{,}640) = 1{,}230$ kips (LRFD)
[= 1,230 kips in AISC Manual (AISC, 2005b)] **o.k.**

One can also compute the associated ASD strength as:

$P_n/\Omega_c = (1640 \text{ kips}/2.00) = 820$ kips (ASD)
[= 821 kips AISC Manual, (AISC, 2005b)] **o.k.**

ANALYSIS OF COMPOSITE SECTIONS FOR COMBINED AXIAL COMPRESSION AND FLEXURAL LOADS

The calculation of the flexural strengths, which follows, is keyed to the stress distributions shown in Table 1. Table 2 shows the applicable formulae for the case of an encased shape (SRC) for strong axis bending and Table 3 those for weak axis bending. Note that in order to keep the tables simple, only some cases are addressed directly. In particular these are cases where continuous reinforcing bars are grouped near the corners of the SRC sections. Modifications to the tables are discussed in the text; for a more general case, see Appendix B in Viest, Colaco, Furlong, Griffis, Leon and Wyllie (1997). Similar tables are given for rectangular concrete-filled tubes (Table 4) and circular concrete-filled sections (Table 5). Note that for Point B in Table 5 changes have been made to the table as it appears in the AISC 13th Ed. *Steel Construction Manual CD Companion* accompanying the AISC *Manual* (AISC, 2005b). These changes correct what appear to be a typographical error in the computation of θ and a discrepancy in the computation of Z_{sB}. The correct expression for θ is

$$\theta = \frac{0.0260K_c - 2K_s}{0.0848K_c} + \frac{\sqrt{(0.0260K_c + 2K_s)^2 + 0.857K_cK_s}}{0.0848K_c}$$

The correct expression for Z_{sB} is

$$Z_{sB} = \frac{d^3 - h^3}{12}\sin^3(\theta/2)\left[\frac{\theta}{\theta - \sin\theta} + \frac{(2\pi - \theta)}{(2\pi-\theta) - \sin(2\pi - \theta)}\right]$$

As shown in Table 5 of this paper, Z_{sB} can be approximated by

$$Z_{sB} \approx \frac{d^3 - h^3}{6}\sin^{(4/3)}(\theta/2)$$

Also note that Tables 4 and 5 for CFTs carry the fifth point (E), which was dropped from the AISC *Manual* tables. Finally these tables also differ from the ones in the CD-Rom in that the intermediate bars at the centroid of the sections are not considered herein.

The generation of axial load-flexure interaction diagrams is a well-documented but tedious procedure (Figure 1), involving the selection of a neutral axis location and a controlling strain (generally 0.003 for the concrete in compression). Assuming a linear distribution of strain (Figure 1b), a corresponding stress distribution can be found based on the stress-strain characteristics assumed for the materials (Figure 1c) and the level of strain (Figures 1d through f). Summing the forces and moments about the assumed reference axis gives a single combination of axial load, P, and moment strength, M. Moving the location of the neutral axis slightly will lead to a different combination of axial load and moment strength, and the interaction surface can be generated by moving the location of the neutral axis methodically (in other words, giving the rounded curves in Figure 3). This is a process that is most easily carried out with the aid of charts, spreadsheets, or subroutines directly embedded within commercial structural analysis software packages.

It is important to recognize some characteristics of diagrams such as that shown in Table 1, particularly the difference between the assumed neutral axis and the reference axis about which moments are calculated. The latter is an arbitrary choice, usually taken at the centroid of the symmetric section. For that case, it is easy to see that insofar as the summation of axial forces is concerned, the contributions of the longitudinal bars and steel flanges in Figure 5 cancel each other out, leaving only the contributions of the web of the steel shape and the rectangular concrete block. Tables 2 through 5 make extensive use of these simplifications, and what may appear to be missing terms in some of the equations shown are actually the result of cancellation of terms as discussed above.

A careful choice of the location of the neutral axis leads to the rapid generation of an interaction surface very close to the more refined one described above through the use of the expressions in these tables. The location of those points is shown in Figure 3, corresponding to the positions in Table 1. Because of the concavity in the curve between Points A and B for the case of minor axis bending of SRC sections, an additional Point E is used.

The four points in Figure 3a and Table 1 correspond to:

- Point A: pure axial load case, with the cross-section under uniform compression corresponding to $\varepsilon_c = 0.003$.
- Point B: pure flexure case, with all steel in tension and compression yielding, ignoring concrete tensile contribution, and $\varepsilon_c = 0.003$. The neutral axis is located at a distance h_n above the centroid.
- Point C: intermediate case, with the neutral axis located at a distance h_n below the centroid. This approach assumes that the interaction diagram (Figure 3a) is roughly symmetrical about the axial load at the balance point (Point D) up to a moment equal to the plastic strength of the section (Point B). Thus Point C has been selected as an arbitrary but convenient point given that it has the same moment as Point B and twice the axial strength of the balance point. This choice considerably simplifies calculations without appreciable error for symmetrical sections.
- Point D: balance point, or point of maximum moment, corresponding to the neutral axis at the centroid as this gives the largest flexure contribution from the concrete portion.

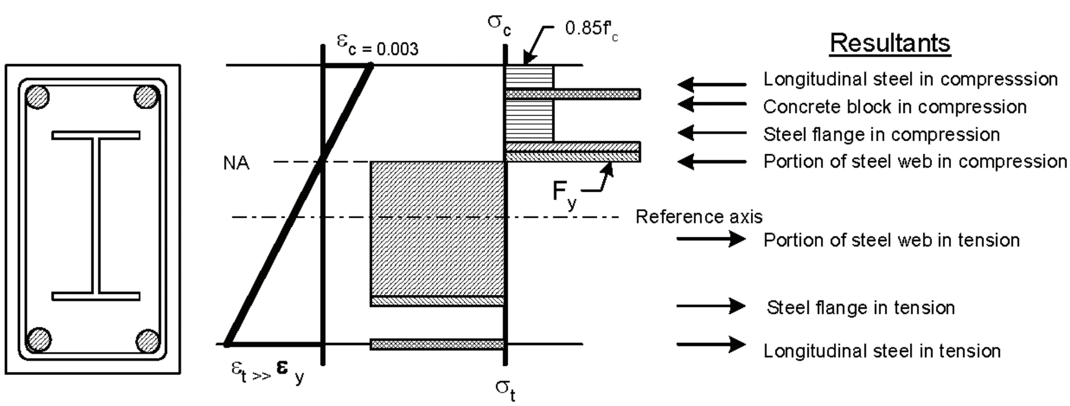

Fig. 5. Calculation of axial load and flexural strength for a given position of the NA.

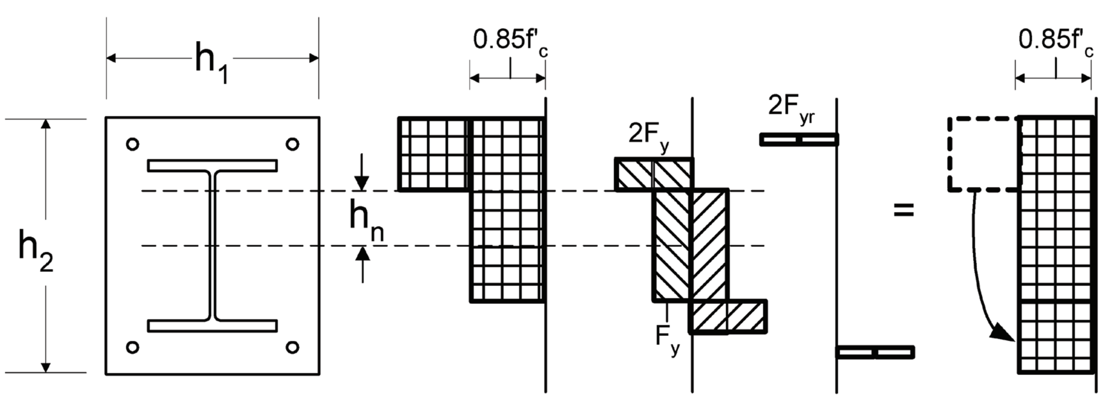

Fig. 6. Axial strength at Point C obtained by adding cases (b) and (c) from Table 1.

The fifth point (Point E), used for SRC bent about its weak axis and concrete-filled tubes (Figure 3b), is computed by selecting an arbitrary position of the neutral axis between Points A and C. For SRC bent about the weak axis, this point is usually taken with the neutral axis at the flange tips.

In the computations that follow, as with the prior examples, the materials are assumed as rigid perfectly-plastic and assumed to have reached high strains so that the elastic contribution is small. The design does not include any explicit checks to ascertain that these large strains can be achieved. It is assumed that the requirements for local buckling and transverse reinforcement implicitly satisfy this requirement. All the steel is assumed to be yielding in tension or compression and strain hardening is ignored. The concrete is assumed to reach its strength at a strain of 0.003, and its nonlinear stress distribution is assumed to be well-represented by an equivalent rectangular block with a stress at $0.85f'_c$. There is currently some discussion of whether this is the best representation for high strength concrete, but this assumption has provided reasonable results for composite columns with concrete strengths up to approximately 10 ksi. The differences in performance between confined and unconfined concrete are ignored, except that for the case of concrete-filled circular pipes, where the stress can be increased from $0.85\,f'_c$ to $0.95f'_c$ as mentioned earlier.

Steel Reinforced Concrete (SRC) Major Axis Bending

The development of the unfactored interaction diagram for a SRC column bent about its major axis (Table 2) requires the following steps (Roik and Bergmann, 1992):

1. Point A is the squash load for the column, P_o, obtained by setting all the materials at their plastic axial strength. Thus:

$$P_A = P_o = A_s F_y + A_{sr} F_{yr} + 0.85 f'_c A_c$$

2. The axial force at Point C is obtained next by adding the stress distributions from Cases (b) and (c) in Table 1 and integrating the resulting stresses across the cross section. The summation is purely a mathematical artifice to obtain the axial load at C, since Case (b) corresponds to the case of no axial load while Case (c) corresponds to the axial load needed for Point C. The resultant stress blocks from this sum are shown in Figure 6.

   As can be seen from Figure 6, all the forces in the steel section and reinforcing bars cancel each other out when computing the resultant axial force, leaving only the concrete portions as the axial force resultant. As only axial force is to be computed using this diagram, it is possible to move the concrete compression block from Case (b) to a location below that of Case (c). Thus the concrete compression area can be represented by a rectangular distribution across the entire section, simplifying the calculation of the axial force:

$$P_C = 0.85 f'_c (h_1 h_2 - A_s - A_{sr}) = \ 0.85 f'_c (h_1 h_2 - A_s - A_{sr})$$

3. The axial force at Point D corresponds to one-half of that at Point C, as the stress blocks corresponding to Point D will result from subtracting an area equal to $h_n\, h_2$ from the axial force at Point C. Subtracting an additional $h_n\, h_2$ from Point D will lead to Point B, in other words, the zero axial load case. Thus:

$$P_D = 0.425 f'_c (h_1 h_2 - A_s - A_{sr}) = 0.425 f'_c A_c$$

$$P_B = 0$$

4. The moment at Point D corresponds to the summation of all plastic section moduli times their yield stress, with the exception that the concrete contribution is halved because only the portion in compression contributes. The moment at Point D is thus:

$$M_D = Z_s F_y + Z_r F_{yr} + \tfrac{1}{2} Z_c \left(0.85 f'_c\right)$$

   where

$$Z_s = \frac{(d-2t_f)\,t_w^2}{4} + b_f\, t_f\,(d - t_f), \text{ or}$$

   or as given in Part 1 of the AISC Manual

$$Z_r = \sum_{i=1}^{R} A_{sr_i} e_i, \text{ where } R \text{ is the total number of bars}$$

$$Z_c = \frac{h_1 h_2^2}{4} - Z_s - Z_r$$

   In these formulas A_{sr_i} is the area of reinforcing bar i and e_i is its distance from the plastic neutral axis.

5. To calculate the moments at B and C, another mathematical trick is used. The stress distribution for Point C is subtracted from that of Point B. Most of the forces cancel out, leading to the stress blocks shown in Figure 7. Because these remaining stress blocks result in a zero net moment about the centroid, the moments at B and C must be equal. In addition, since we know from Step 2 (above) what the value of P_C is, the distribution shown in Figure 7 allows the value of h_n to be calculated. In the calculations for Figure 7, the steel stress is decreased by $0.85f'_c$ for consistency with the uniform stress used in Step 2. In addition, one must check that $h_n < (d/2 - t_f)$ to insure that the location of h_n is within the web of the steel section. Finally, note that there are no reinforcing

bars within the $2h_n$ zone near the middle of the beams; if there were, the force in those bars, equal to $A_{sr}(2F_{yr}\text{-}0.85f_c')$, must be subtracted from the numerator of the expression for h_n. Thus:

$$M_C = M_B$$

$$P_C = 0.85f_c'A \quad \text{(from Step 2)}$$

$$P_C = 2h_n\left(0.85f_c'h_1 + t_w(2F_y - 0.85f_c')\right) \quad \text{(from Figure 7)}$$

$$h_n = \frac{0.85f_c'h_1h_2}{2(0.85f_c'h_1 + t_w(2F_y - 0.85f_c'))} \leq \left(\frac{d}{2} - t_f\right)$$

6. Once h_n has been obtained, the moments at B and C can be calculated using either of the given stress distributions. Alternatively, this moment can be obtained by subtracting the contribution of the portions within the central $2h_n$ region from the maximum moment (M_D). Thus:

$$M_C = M_B = M_D - Z_{sn}F_y - ½Z_{cn}(0.85f_c')$$

$$Z_{sn} = t_wh_n^2$$

$$Z_{cn} = h_1h_n^2 - Z_{sn}$$

$$Z_r = \sum_{i=1}^{N} A_{s\,r_i}e_i, \text{ where } N \text{ is the number of bars within } 2h_n$$

7. If step (5) resulted in the location of h_n not being in the web, the next assumption is that it will be within the flange. For this case, the expressions for h_n and Z_s become:

$$h_n = \frac{0.85f_c'\left(A_c + A_s - db_f\right) - 2F_y\left(A_s - db_f\right)}{2\left[0.85f_c'\left(h_1 - b_f\right) + 2F_yb_f\right]}$$

$$Z_{sn} = Z_s - b_f\left(\frac{d}{2} - h_n\right)\left(\frac{d}{2} + h_n\right), \frac{d}{2} - t_f \leq h_n \leq \frac{d}{2}$$

8. Finally, if the location of h_n is outside the steel shape, the expressions for h_n and Z_s become:

$$h_n = \frac{0.85f_c'\left(A_c + A_s\right) - 2F_yA_s}{2\left(0.85f_c'h_1\right)}$$

$$Z_{sn} = Z_{sx}$$

Steel Reinforced Concrete (SRC) Minor Axis Bending

The procedure for determining the axial load-flexure interaction diagram for minor axis bending is the same as that for major axis bending with two exceptions:

1. There are only two possible locations of h_n (either within or outside the steel section – see Table 3).

2. Another location of h_n is needed to determine Point E. A convenient location to choose is the tip of the flanges. This is the case shown in Table 3 as Point E. The expressions derived for the cases where the plastic neutral axis is within the steel section (Points B and C) are valid for the calculation of the values at Point E, except that $h_n = b_f/2$.

Rectangular Concrete-Filled Steel Tube (RCFT)

The procedure for determining the axial load-flexure interaction diagram for rectangular concrete-filled tubes is similar to that described above for SRC, and the resulting values are shown in Table 4.

Circular Concrete-Filled Steel Tube (CCFT)

The resulting values for CCFT sections are shown in Table 5. Note again that in the definitions of θ and Z_s for Point B, changes have been made to correct errors in the table that appear in the AISC 13th Ed. *Steel Construction Manual CD Companion* accompanying the AISC *Manual* (AISC, 2005b).

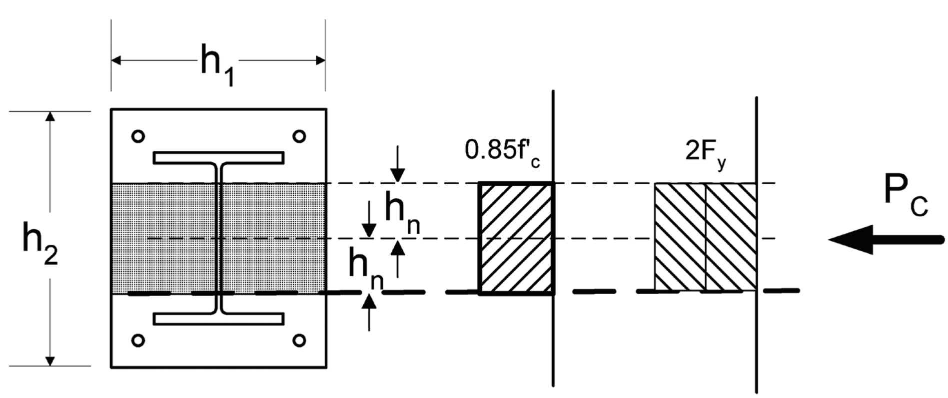

Fig. 7. Moment at Points B and C: stress resultants corresponding to the subtraction of cases (b) and (c) in Table 1 and leading to the calculation of h_n.

STABILITY CONSIDERATIONS

Once the cross-sectional strength has been established, this interaction surface needs to be reduced to account for: (a) stability effects and (b) design strength as opposed to nominal strength. To account for stability, the usual column formula has been used in conjunction with an equivalent moment of inertia. This is straightforward, although it results in a substantial difference in the approach to stability from that given, for example, in ACI 318 (ACI, 2005) for composite columns. The next step, the reduction from nominal to design loads, is not so simple due to the fact that as the failure shifts from tension yielding at low axial loads to compression at loads above the balance point, it will seem that the overall factor for the member should change. In reinforced concrete design this is achieved by changing the resistance factor from 0.90 to 0.65 as the strain in the extreme tensile fiber goes from 0.0005 to the yield strain of the steel. This factor is applied to both the moment and axial force components. AISC has chosen not to use that approach and to retain separate resistance factors and safety factors for axial loads and flexure. This, and the desire to provide simplified approaches for design, has resulted in three separate approaches to checking the strength of a composite beam-column: (1) an approach based on the use of the existing interaction formulas in AISC 2005 *Specification* Chapter H (AISC, 2005a); (2) a more complex approach based on the complete polygonal interaction diagram; and (3) a simplified version of the polygonal approach that uses only one intermediate point. A description of these approaches follows.

Method 1: Approach Based on AISC 2005 Chapter H

For this case, only the nominal axial strength including stability effects, P_n, and the nominal flexural strength of the section, M_n, need to be computed. This makes this approach particularly useful for biaxial bending cases where the engineer does not want to compute additional interaction points for combined axial force and flexure. The anchor points (for uniaxial flexure) can be based on the equations for Points A and B given in Tables 2 through 5, with the stability reduction included in P_n. The interaction Equations H1-1a and H1-1b from Chapter H (AISC, 2005a) are then used directly (Figure 8):

(a) For $\dfrac{P_r}{P_c} \geq 0.2$

$$\frac{P_r}{P_c} + \left(\frac{M_{rx}}{M_{cx}} + \frac{M_{ry}}{M_{cy}}\right) \leq 1.0 \qquad \text{(AISC H1-1a)}$$

(b) For $\dfrac{P_r}{P_c} < 0.2$

$$\frac{P_r}{2P_c} + \left(\frac{M_{rx}}{M_{cx}} + \frac{M_{ry}}{M_{cy}}\right) \leq 1.0 \qquad \text{(AISC H1-1b)}$$

where

P_r = required compressive strength, kips (N)
P_c = available compressive strength, kips (N)
M_r = required flexural strength, kip-in. (N-mm)
M_c = available flexural strength, kip-in. (N-mm)
x = subscript relating symbol to strong axis bending
y = subscript relating symbol to weak axis bending

For this case, the safety and resistance factors from Section I4 are applicable:

$\phi_c = 0.75$ (LRFD) $\quad \Omega_c = 2.00$ (ASD)

$\phi_b = 0.90$ (LRFD) $\quad \Omega_b = 1.67$ (ASD)

Similar equations may be used for the case of axial tension plus flexure.

Method 2: Full Plastic Strength Approach Based on Polygonal Interaction Envelope

This approach requires the calculation of the full interaction diagram or a reduced set thereof (for example, the four or five points shown in Tables 2 through 5). The axial load values

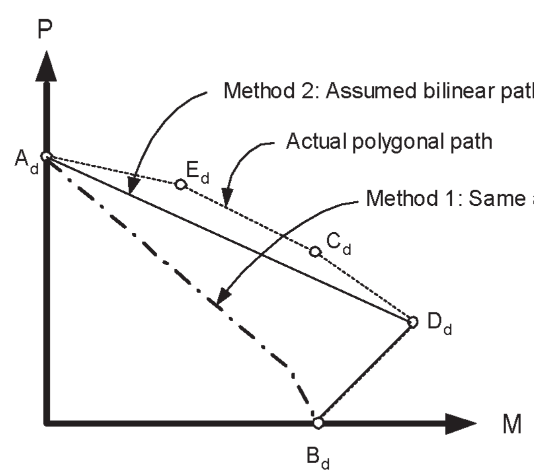

Fig. 8. Schematic representations of Methods 1 and 2 for checking axial load and flexure interaction.

are then reduced to take into account stability effects and also reduced by the following safety and resistance factors:

$\phi_c = 0.75$ (LRFD) $\Omega_c = 2.00$ (ASD)

$\phi_b = 0.90$ (LRFD) $\Omega_b = 1.67$ (ASD)

The corresponding interaction diagram is shown in Figure 8, where the subscript d indicates that the values are the design ones (in other words, including a slenderness reduction and the resistance factor). The number of checks and equations needed increase substantially as the number of points used to define the envelope increases. The complete set of equations needed for the case of checking the resistance between the five points is too lengthy to be included here and thus only a simplified case will be illustrated. For a possible polygonal approach to the interaction diagram using Points A, B, and D only, the checks then become:

If $P_n < P_D$

and if $\dfrac{M_{rx}}{M_{cx}} \le 1$ and $\dfrac{M_{ry}}{M_{cy}} \le 1$ then

$$\frac{M_{rx}}{M_{cx}} + \frac{M_{ry}}{M_{cy}} \le 1 \tag{1}$$

otherwise if $\dfrac{M_{rx}}{M_{cx}} > 1$ and $\dfrac{M_{ry}}{M_{cy}} \le 1$ then

$$\frac{P_r}{P_{cb}} + \frac{M_{cbx} - M_{rx}}{M_{cbx} - M_{cx}} + \frac{M_{ry}}{M_{cy}} \le 1 \tag{2}$$

otherwise if $\dfrac{M_{rx}}{M_{cx}} \le 1$ and $\dfrac{M_{ry}}{M_{cy}} > 1$ then

$$\frac{P_r}{P_{cb}} + \frac{M_{rx}}{M_{cx}} + \frac{M_{cby} - M_{ry}}{M_{cby} - M_{cy}} \le 1 \tag{3}$$

otherwise if $\dfrac{M_{rx}}{M_{cx}} > 1$ and $\dfrac{M_{ry}}{M_{cy}} > 1$ then

$$\frac{P_r}{P_{cb}} + \frac{M_{cbx} - M_{rx}}{M_{cbx} - M_{cx}} + \frac{M_{cby} - M_{ry}}{M_{cby} - M_{cy}} \le 1 \tag{4}$$

If $P_r \ge P_{cb}$

$$\frac{P_r - P_{cb}}{P_c - P_{cb}} + \frac{M_{rx}}{M_{cbx}} + \frac{M_{ry}}{M_{cby}} \le 1 \tag{5}$$

where

P_r = required compressive strength, kips (N)
P_c = available compressive strength, kips (N)
P_{cb} = axial compressive strength at balanced moment, M_{cb}, kips (N)
M_r = required flexural strength, kip-in. (N-mm)
M_c = available flexural strength, kip-in. (N-mm)
M_{cb} = balanced moment, kip-in. (N-mm)
x = subscript relating symbol to strong axis bending
y = subscript relating symbol to weak axis bending

Similar equations as those given for Method 1 may be used for the case of axial tension plus flexure.

One issue with using a different set of resistance and safety factors for flexure and axial force is the possibility that upon the application of the stability reduction coupled with the resistance or safety factors, the resulting available strength envelope may fall outside the cross section strength envelope in the area immediately below the balance point (Figure 9). A simple way has not yet been determined for including this added strength without encountering this potential unconservative design area within the context of accounting for stability using the current AISC *Specification*.

Method 3: Simplified Approach Based on Polygon Values

To maintain some of the substantial strength gains from the strain compatibility approach but to simplify the design process, a third approach has been proposed. In this approach, a third anchor point, C_d, is used in addition to points A_d and B_d as seen in Figure 10. The new Point C_d is derived from the flexural design strength of the member (M_n from Point B) and the corresponding axial strength from Point C (See Figure 3), with appropriate reduction taken to account for slenderness effects and resistance or safety factors as per Leon et al. (2007). Similar equations as those given for Method 2 may be used for the case of axial tension plus flexure.

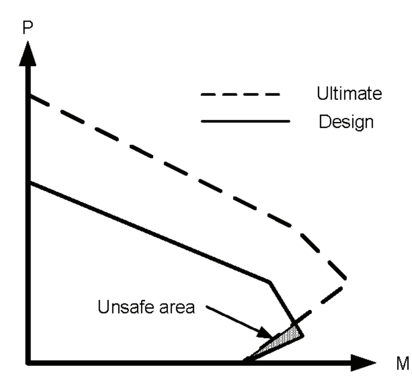

Fig. 9. Possible breaching of ultimate strength envelope by design envelope due to application of resistance and stability reduction factors.

Design Examples

Example 3: SRC Beam-Column

In this example, a simplified axial load-moment envelope is developed for an 18 in. × 18 in. SRC beam-column with an embedded W14×48 section. Additional reinforcement consists of four #7 corner bars and #3 ties spaced at 12 in. Materials used include F_y = 50 ksi, F_{yr} = 60 ksi, and f_c' = 3 ksi. Flexure is about the major axis, the effective length is 24 ft, and buckling is restrained about the minor axis.

Limitations:

1) Normal weight concrete 10 ksi $\geq f_c' \geq$ 3 ksi; in this case f_c' = 3 ksi **o.k.**

2) $F_{yr} \leq$ 75 ksi; in this case, F_{yr} = 60 ksi **o.k.**

3) The cross-sectional area of the steel core shall comprise at least 1% of the total composite cross section.

   A_s = 14.1 in.^{2} > (0.01)(324 in.^{2}) = 3.24 in.^{2} **o.k.**

4) Concrete encasement of steel core shall be reinforced with continuous longitudinal bars and lateral ties or spirals. The minimum transverse reinforcement shall be at least 0.009 in.^{2} of tie spacing:

   ρ_{st} = 0.22 in.^{2}/12 in. = 0.0183 in.^{2}/in. > 0.009 in.^{2}/in. **o.k.**

5) The minimum steel ratio for continuous longitudinal reinforcing, ρ_{sr}, shall be 0.004:

$$\rho_{sr} = \frac{A_{sr}}{A_g} = \frac{(4 \times 0.6)}{324} = 0.0074 > 0.004 \textbf{ o.k.}$$

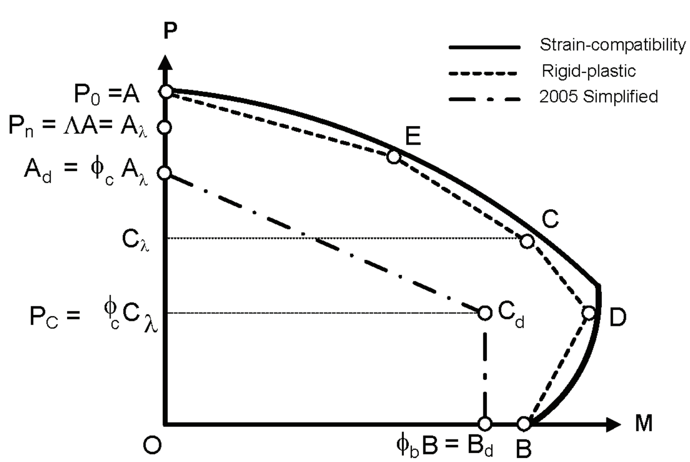

Fig. 10. Simplified interaction diagram for LRFD design.

Point A in Table 2 (M = 0)

Determine the available compressive strength and moment strength.

$$A_c = (324 - 14.1 - 2.40) = 308 \text{ in.}^2$$

$$P_o = A_s F_y + A_{sr} F_{yr} + 0.85 A_c f_c'$$

$$P_o = (14.1)(50) + (2.40)(60) + 0.85(308)(3) = 1{,}630 \text{ kips}$$

$$C_1 = 0.1 + 2\left(\frac{A_s}{A_c + A_s}\right) = 0.1 + 2\left(\frac{14.1}{308 + 14.1}\right) = 0.188 \leq 0.3$$

$$e_1 = \left(\frac{\text{overall depth} - 2\text{ (cover)} - 2\text{(stirrup)} - \text{bar diameter}}{2}\right)$$

$$e_1 = \left(\frac{18 - (2)(1.5) - (2)(0.375) - 0.875}{2}\right) = 6.69 \text{ in.}$$

$$I_{sr} \approx \sum \left(A_{sr_i}\right)(e_i)^2 = 2(1.20)(6.69)^2 = 107 \text{ in.}^3$$

$$I_c = \left(\frac{h_1 h_2^3}{12}\right) - I_s - I_{sr}$$

$$= \left(\frac{(18)(18)^3}{12}\right) - 484 - 107 = 8{,}160 \text{ in.}^4$$

$$E_c = \left(148.1 \text{ lb/ft}^3\right)^{1.5} \sqrt{3 \text{ ksi}} = 3{,}122 \text{ ksi}$$

$$EI_{eff} = E_s I_s + 0.5 E_s I_{sr} + C_1 E_c I_c$$

$$EI_{eff} = (29{,}000)(484) + (0.5)(29{,}000)(107) + (0.188)(3{,}122)(8{,}160)$$

$$EI_{eff} = 20.4 \times 10^6 \text{ kip-in.}^2$$

Note that if buckling had not been prevented about the minor axis, the I_s to be used in the computation of I_{eff} would have been I_y rather than I_x.

$$P_e = \frac{\pi^2 EI_{eff}}{(kL)^2} = \frac{\pi^2 (20.4 \times 10^6)}{(24 \times 12)^2} = 2{,}430 \text{ kips}$$

$$\frac{P_o}{P_e} = \frac{1{,}630}{2{,}430} = 0.67 \leq 2.25$$

or

$$\frac{P_e}{P_o} = \frac{2{,}430}{1{,}630} = 1.49 > 0.44$$

∴ Use Equation (AISC 2005 I2-2)

$$P_n = P_o\left[0.658^{\left(\frac{P_o}{P_e}\right)}\right] = (1{,}630 \text{ kips})\left[0.658^{(0.67)}\right] = 1{,}230 \text{ kips}$$

$\phi_c P_n = (0.75)(1{,}230) = 923$ kips (LRFD)

$P_n/\Omega_c = (1{,}230 \text{ kips}/2.00) = 615$ kips (ASD)

Point B in Table 2 ($P_B = 0$)

Determine the location of h_n

1) Above the flange or $\left(h_n > \dfrac{d}{2} = \dfrac{13.8 \text{ in.}}{2}\right) = h_n > 6.90$ in.

$$h_n = \frac{0.85f_c'\left(A_c + A_s\right) - 2F_yA_s}{2\left(0.85f_c'h_1\right)}$$

$$= \frac{0.85\left(3.0\right)\left(308 + 14.1\right) - 2\left(50\right)\left(14.1\right)}{2\left(0.85\right)\left(3.0\right)\left(18\right)}$$

$= -6.41$ in. < 6.90 in., so h_n is not outside the steel section

2) For h_n within the flange $\left[\left(\dfrac{d}{2} - t_f\right) < h_n \le \dfrac{d}{2}\right]$

or 6.31in.$< h_n \le 6.90$ in.

$$h_n = \frac{0.85f_c'\left(A_c + A_s - db_f\right) - 2F_y\left(A_s - db_f\right)}{2\left[0.85f_c'\left(h_1 - b_f\right) + 2F_yb_f\right]}$$

$$= \frac{\left[0.85(3)\left(308 + 14.1 - (13.8)(8.03)\right)\right]}{2\left[0.85(3)\left(18 - 8.03\right) + 2(50)(8.03)\right]}$$

$$- \frac{\left[2(50)\left(14.1 - (13.8)(8.03)\right)\right]}{2\left[0.85(3)\left(18 - 8.03\right) + 2(50)(8.03)\right]}$$

$= 6.16$ in., so h_n is in the web

Since h_n is within the web and thus no rebars are present within h_n ($A_{sr} = 0$):

$$h_n = \frac{0.85f_c'A_c}{2\left[0.85f_c'\left(h_1 - t_w\right) + 2F_yt_w\right]}$$

$$= \frac{0.85\left(3\right)(308)}{2\left[0.85(3)\left(18 - 0.340\right) + 2(50)(0.340)\right]}$$

$= 4.96$ in.

$Z_{sn} = t_wh_n^2 = (0.340)(4.96)^2 = 8.36 \text{ in.}^3$

$Z_{cn} = h_1h_n^2 - Z_{sn} = (18)(4.96)^2 - 8.37 = 434 \text{ in.}^3$

Before computing M_b, M_D must be computed:

$M_D = Z_sF_y + Z_rF_{yr} + ½Z_c\left(0.85f_c'\right)$

$Z_r = \sum A_{sr_i}\left(\dfrac{h_2}{2} - c\right) = \sum\left(A_{sr_i}e_i\right) = 4(0.6)(6.69)$

$= 16.1 \text{ in.}^3$

$Z_c = \left(\dfrac{h_1h_2^2}{4}\right) - Z_s - Z_r = \left(\dfrac{(18)(18)^2}{4}\right) - 78.4 - 16.1$

$= 1{,}360 \text{ in.}^3$

$M_D = (78.4)(50) + (16.1)(60) + ½(1{,}360)\left(0.85)(3\right)$

$= 6{,}620$ kip-in.

$M_B = M_D - Z_{sn}F_y - ½Z_{cn}\left(0.85f_c'\right)$

$= (6{,}620) - (8.36)(50) - ½(434)(0.85)(3)$

$= 5{,}650$ kip-in.

$\phi_b M_B = (0.90)(5{,}650) = 5{,}090$ kip-in.

$M_B/\Omega_b = (5{,}650/1.67) = 3{,}380$ kip-in.

Point C ($M_C = M_B$; $P_C = 0.85 f_c'A_c$)

$P_C = A_c\left(0.85f_c'\right)$

$= \left(308 \text{ in.}^2\right)\left(0.85\right)\left(3.0 \text{ ksi}\right) = 785$ kips

$\phi P_{C_d} = 0.75(785)(0.658)^{0.67} = 445$ kips

$P_{C_d}/\Omega = (784)(0.658)^{0.67}/2.00 = 296$ kips

$M_C = M_B = 5{,}650$ kip-in.

$\phi M_C = \phi M_B = (0.9)5{,}650$ kip-in. $= 5{,}090$ kip-in.

$M_C/\Omega = M_B/\Omega = 5{,}650/1.67$ kip-in. $= 3{,}380$ kip-in.

Point D

$$P_D = \frac{A_c\left(0.85f_c'\right)}{2}$$

$$= \frac{\left(308 \text{ in.}^2\right)\left(0.85\right)\left(3.0 \text{ ksi}\right)}{2}$$

$= 393$ kips

$\phi P_{D_d} = 0.75(393)(0.658)^{0.67} = 223$ kips

$P_{D_d}/\Omega = (393)(0.658)^{0.67}/2.00 = 148$ kips

$M_D = 6{,}620$ kip-in.

$\phi M_D = (0.9)6{,}620 = 5{,}960$ kip-in.

$M_D/\Omega = 6{,}620/1.67 = 3{,}960$ kip-in.

The results are summarized in Figure 11.

Example 4: RCFT Beam-Column

Develop a simplified axial load-moment envelope for a HSS16 in.×16 in.×⅝ in. filled with $f_c' = 4$ ksi concrete. The effective length of the member is 24 ft. Assume A500 Grade B ($F_y = 46$ ksi and $F_u = 58$ ksi). Note that the design thickness for a 0.625 in. nominal value is 0.581 in.

Limitations:

1) The cross-sectional area of the steel core shall comprise at least 1% of the total composite cross-section.

$A_s = 35.0 \text{ in.}^2 > (0.01)(16)^2 = 2.56 \text{ in.}^2$ **o.k.**

Note that $\rho = \dfrac{35}{256} = 0.137$, or 13.7% which is very high.

2) The slenderness of the tube wall is:

$$\left(\frac{b}{t}\right) = \frac{16(2)(0.581)}{0.581}$$

$$= 25.5 < 2.26\sqrt{\frac{E}{F_y}} = 2.26\sqrt{\frac{29{,}000}{46}} = 56.7 \textbf{ o.k.}$$

Point A in Table 4 ($M_A = 0$)

Determine the available compressive strength and flexural strength.

In the following calculations the symbol "≈" is used to indicate that the effect of the corner radii is not being accounted for exactly; this effect is small and can generally be neglected.

$$P_o = A_s F_y + A_{sr} F_{yr} + 0.85 A_c f_c'$$

$$A_c \approx 256 - 35.0 = 221 \text{ in.}^2$$

$$P_o = (35.0)(46) + 0.85(221)(4)$$

$$= 2{,}360 \text{ kips}$$

$$C_3 = 0.6 + 2\left(\frac{A_s}{A_c + A_s}\right) = 0.6 + 2\left(\frac{35}{(221+35)}\right)$$

$$= 0.873$$

$$I_s = 1{,}370 \text{ in.}^4$$

$$I_c \approx \left(\frac{d^4}{12}\right) - I_s = \left(\frac{(16)^4}{12}\right) - 1{,}370 = 4{,}090 \text{ in.}^4$$

$$E_c = (148.1 \text{ lb/ft}^3)^{1.5}\sqrt{4 \text{ ksi}} = 3{,}605 \text{ ksi}$$

SRC: 18x18, W14×48, 4-#7 bars, $f_c' = 3$ ksi, $F_y = 50$ ksi, $KL = 24$ ft

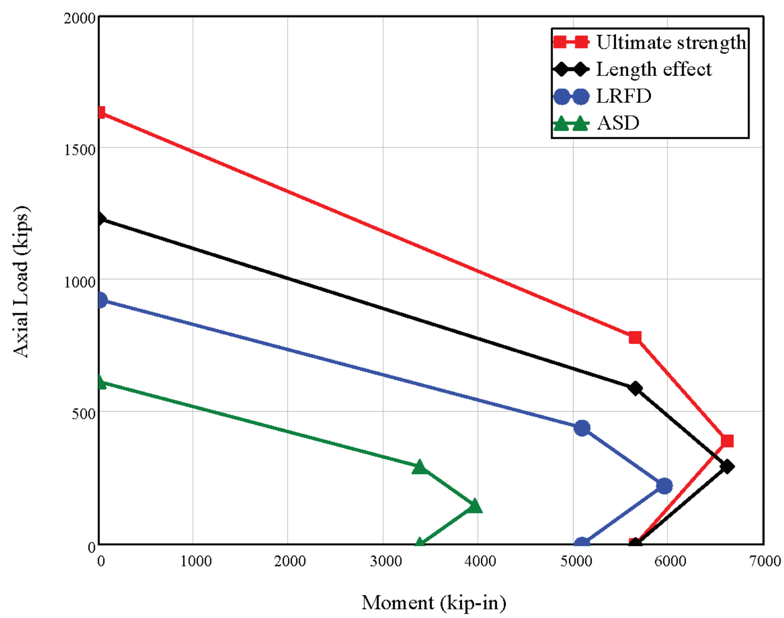

Fig. 11. Interaction diagrams for column in Example 3.

$$EI_{eff} = E_s I_s + 0.5 E_s I_{sr} + C_3 E_c I_c$$
$$= (29,000)(1,370) + (0.873)(3,605)(4,090)$$
$$= 52.6 \times 10^6 \text{ kip-in.}^2$$

$$P_e = \frac{\pi^2 EI_{eff}}{(KL)^2} = \frac{\pi^2 (52.6 \times 10^6)}{(24 \times 12)^2} = 6,260 \text{ kips}$$

$$\frac{P_o}{P_e} = \frac{2,360}{6,260} = 0.38 < 2.25$$

$$\text{or } \frac{P_e}{P_0} = \frac{6,260}{2,360} = 2.65 > 0.44$$

∴ Use Equation (AISC 2005 I2-2)

$$P_n = P_o \left[0.658^{\left(\frac{P_o}{P_e}\right)} \right] = (2,360)\left[0.658^{(0.38)}\right]$$

$$= 2,010 \text{ kips}$$

$\phi_c P_n = (0.75)(2,010) = 1,510$ kips (LRFD)

$P_n/\Omega_c = (2,010/2.00) = 1,010$ kips (ASD)

Point B in Table 4 ($P_B = 0$)

Determine location of h_n

$$h_n = \frac{0.85 f_c' A_c}{2\left[0.85 f_c' h_1 + 4 t_w F_y\right]} \le \frac{h_2}{2}$$

$$= \frac{0.85(4)(221)}{2\left[0.85(4)[16-(2)(0.581)] + 4(0.581)(46)\right]}$$

$$= 2.39 \text{ in.} \le \frac{(16-(2)(0.581))}{2} = 7.42 \text{ in.}$$

Before computing M_B, M_D must be computed.

$Z_s = 200$ in.^{3}

$$Z_c = \frac{h_1 h_2^2}{4} - 0.192 r_i^3 \approx \left(\frac{\left[\left(16-(2)(0.581)\right)\right]^3}{4} \right) = 817 \text{ in.}^3$$

$$M_D = Z_s F_y + \tfrac{1}{2} Z_c \left(0.85 f_c'\right)$$
$$= (200)(46) + \tfrac{1}{2}(817)(0.85 \times 4)$$
$$= 10,600 \text{ kip-in.}$$

$$Z_{sn} = 2 t_w h_n^2 = 2(0.581)(2.39)^2 = 6.64 \text{ in.}^3$$

$$Z_{cn} = h_1 h_n^2 = [16-(2)(0.581)](2.39)^2 = 84.8 \text{ in.}^3$$

$$M_B = M_D - Z_{sn} F_y - \tfrac{1}{2} Z_{cn}\left(0.85 f_c'\right)$$
$$= 10,600 - (6.64)(46) - \tfrac{1}{2}(84.8)(0.85)(4)$$
$$= 10,200 \text{ kip-in.}$$

$\phi_b M_B = (0.9)(10,200) = 9,180$ kip-in.

$M_B/\Omega_b = (10,200/1.67) = 6,110$ kip-in.

Point C in Table 4 ($M_C = M_B$; $P_C = 0.85 f_c' A_c$)

$$P_C = A_c\left(0.85 f_c'\right)$$
$$P_C = \left(221 \text{ in.}^2\right)(0.85)(4.0 \text{ ksi}) = 751 \text{ kips}$$
$$\phi P_{C_d} = (0.75)(751)(0.658)^{0.38} = 480 \text{ kips}$$
$$P_{C_d}/\Omega = 751(0.658)^{0.38}/2.00 = 320 \text{ kips}$$
$$M_C = M_B = 10,200 \text{ kip-in.}$$
$$\phi M_C = (0.9)(10,200) = 9,180 \text{ kip-in.}$$
$$M_C/\Omega = 10,200/1.67 = 6,110 \text{ kip-in.}$$

Point D in Table 4

$$P_D = \frac{A_c\left(0.85 f_c'\right)}{2}$$
$$= \frac{(221)(0.85)(4.0 \text{ ksi})}{2}$$
$$= 376 \text{ kips}$$
$$\phi P_{D_d} = (0.75)(376)(0.658)^{0.38} = 241 \text{ kips}$$
$$P_{D_d}/\Omega = (376)(0.658)^{0.38}/2.00 = 160 \text{ kips}$$
$$M_D = 10,600 \text{ kip-in.}$$
$$\phi M_D = (0.9)(10,600) = 9,540 \text{ kip-in.}$$
$$M_D/\Omega = 10,600/1.67 = 6,350 \text{ kip-in.}$$

The results are summarized in Figure 12.

Example 5: CCFT Beam-Column

Determine the interaction diagram for a 20 in. diameter, ⅜ in. thick circular concrete-filled tube column with a $KL = 13$ ft. Assume $F_y = 42$ ksi and $f_c' = 5$ ksi.

Basic geometrical properties:

$d = 20$ in.

$t = 0.349$ in.

$h = d - 2t = 19.3$ in.

$$r_m = \frac{d-t}{2} = 9.83 \text{ in}$$

$$A_s = 2\pi r_m t = 21.6 \text{ in.}^2$$

$$A_c = \frac{\pi h^2}{4} = 293 \text{ in.}^2$$

$$A_g = A_c + A_s = 315 \text{ in.}^2$$

$$E_c = (148.1)^{1.5}\sqrt{5} = 4{,}030 \text{ ksi}$$

$$I_s = \frac{\pi}{64}\left[d^4 - h^4\right] = 1{,}040 \text{ in.}^4$$

$$I_c = \frac{\pi h^4}{64} = 6{,}810 \text{ in.}^4$$

$$I_g = I_s + I_c = 7{,}850 \text{ in.}^4$$

The cross-sectional area of the steel core shall comprise at least 1% of the total composite cross-section.

$$\frac{A_s}{A_c + A_s} = 0.07 > 0.010 \quad \textbf{o.k.}$$

The slenderness of the tube wall is:

$$\frac{D}{t} = 57.3 < 0.15\left(\frac{E_s}{F_y}\right) = 104 \quad \textbf{o.k.}$$

Point A in Table 5 ($M_A = 0$)

Determine the available compressive strength using the properties determined above.

$C_2 = 0.95$

$$C_3 = \min\left[0.9,\ 0.6 + 2\left(\frac{A_s}{A_c + A_s}\right)\right] = 0.74$$

$$EI_{eff} = E_sI_s + E_sI_{sr} + C_3E_cI_c = 351{,}000 \text{ kip-ft}^2$$

$$P_o = A_sF_y + A_{sr}F_{yr} + C_2A_cf_c' = 2{,}300 \text{ kips}$$

$$P_e = \frac{\pi^2 EI_{eff}}{(KL_c)^2} = 20{,}500 \text{ kips}$$

$$\frac{P_o}{P_e} = \frac{2{,}300}{20{,}500} = 0.112$$

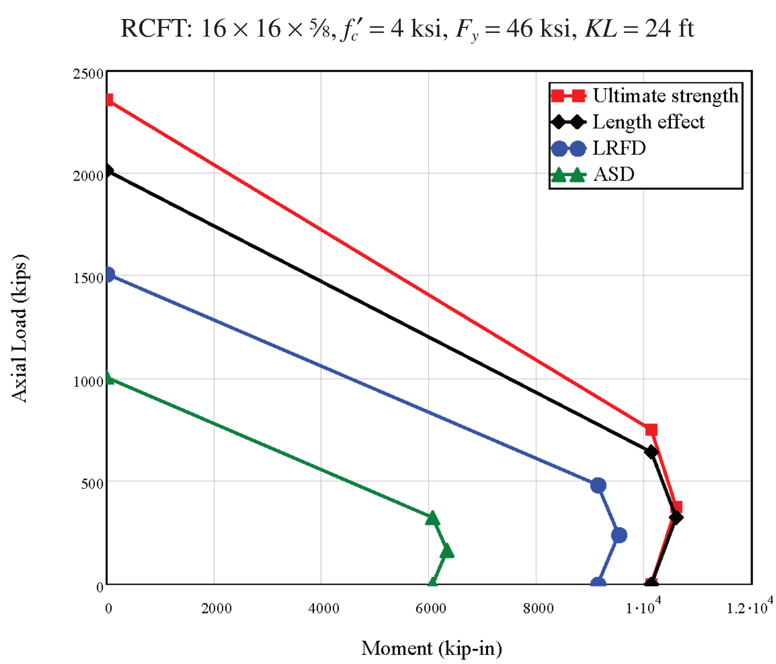

Fig. 12. Interaction diagrams for column in Example 4.

If $P_e > 0.44P_o$, $P_n = \left(0.658^{\frac{P_o}{P_e}}\right)P_o = 2{,}190$ kips

$\phi_c P_n = (0.75)(2{,}190) = 1{,}640$ kips

$P_n/\Omega_c = (2{,}190 \text{ kips}/2.00) = 1{,}100$ kips

Point B in Table 5 ($P_B = 0$)

From definitions of Point B in Table 5:

$K_c = f_c' h^2 = 1{,}860$ kips

$K_s = F_y r_m t = 144$ kips

$$\theta = \frac{0.0260K_c - 2K_s}{0.0848K_c} + \frac{\sqrt{\left(0.0260K_c + 2K_s\right)^2 + 0.857K_cK_s}}{0.0848K_c}$$

$= 2.19$ rad

$$Z_{cB} = \frac{h^3 \sin^3\left(\theta/2\right)}{6} = 842 \text{ in.}^3$$

$$Z_{sB} \approx \frac{d^3 - h^3}{6} \sin^{(4/3)}\left(\theta/2\right) = 116 \text{ in.}^3$$

$$M_B = Z_{sB}F_y + \frac{Z_{cB}\left(0.95f_c'\right)}{2} = 6{,}870 \text{ kip-in.}$$

$\phi_b M_B = (0.9)(6{,}870) = 6{,}180$ kip-in.

$M_B/\Omega_b = (6{,}870/1.67) = 4{,}110$ kip-in.

Point C in Table 5

$P_C = 0.95 f_c' A_c = 1{,}390$ kips

$M_C = M_B = 6{,}870$ kip-in.

Slenderness reductions on the axial strength and application of resistance and safety factors to axial and flexural strength should be taken as per Example 4 and Leon et al. (2007).

Point D in Table 5

$$P_D = \frac{\left(0.95f_c'\right)A_c}{2} = 696 \text{ kips}$$

$$Z_c = h^3/6 = 1{,}200 \text{ in.}^3$$

$$Z_s = \left(d^3/6\right) - Z_c = 133 \text{ in.}^3$$

$$M_D = Z_sF_y + \frac{Z_c\left(0.95f_c'\right)}{2} = 8{,}440 \text{ kip-in.}$$

Slenderness reductions on the axial strength and application of resistance and safety factors to axial and flexural strength should be taken as per Example 4 and Leon et al. (2007).

The results are summarized in Figure 13.

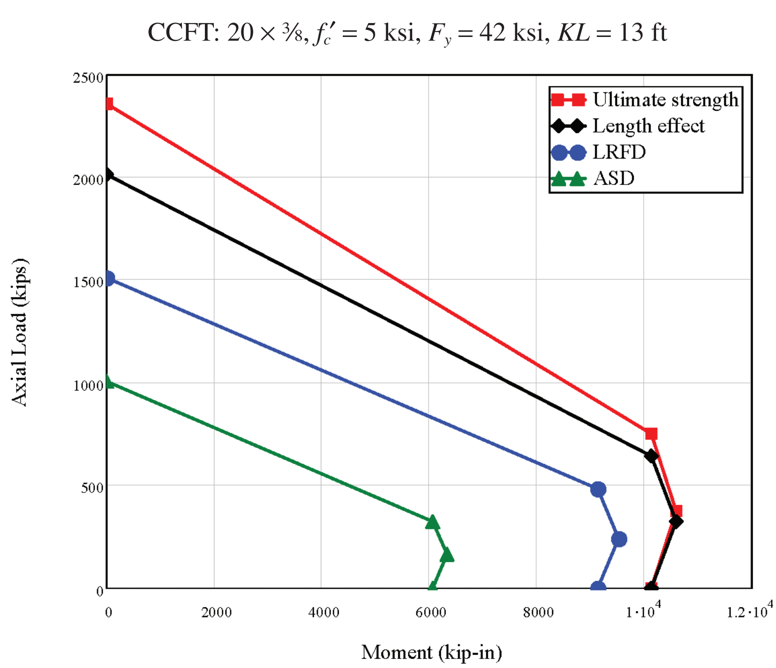

Fig. 13. Interaction diagrams for column in Example 5.

CONCLUSIONS

This paper presents the background on the step-by-step procedures available in the 2005 AISC *Specification* (AISC, 2005a) for computing composite column and beam-column strength, including accounting for stability effects on members subjected to biaxial flexure plus axial compression. The new procedures highlighted in the 2005 AISC *Specification* are discussed, including the use of a plastic stress distribution method that accounts for the beneficial effects of the concrete to the strength of the cross-section. Several examples are given for calculating the design strength of encased composite sections (SRC) as well as filled composite sections, both rectangular (RCFT) and circular (CCFT).

ACKNOWLEDGMENTS

This research was sponsored by the National Science Foundation under Grant No. CMS-0084848, the American Institute of Steel Construction, the Georgia Institute of Technology, the University of Minnesota, and the University of Illinois at Urbana-Champaign. The authors would like to thank the members of AISC Specification Task Committee 5 on Composite Construction for their contributions to this research. The assistance of Tiziano Perea, Cenk Tort, Matthew Eatherton, Arvind Goverdhan and William Jacobs with verifying the design examples is gratefully acknowledged.

APPENDIX A

NOMENCLATURE

A_s = area of the steel section, in.^{2} (mm^2)

A_c = area of concrete, in.^{2} (mm^2) $= A_{gross} - A_s - A_{sr}$

A_{sr} = area of continuous longitudinal reinforcing bars, in.^{2} (mm^2)

A_{sr} = area of a longitudinal bar, in.^{2} (mm^2)

A_{srn} = area of longitudinal bars within the $2h_n$ region, in.^{2} (mm^2)

A_{gross} = total area of member, in.^{2} (mm^2) $= h_1 h_2$

b_f = flange width, in. (mm)

c = cover to centroid of longitudinal bars, in. (mm)

d = depth of steel section, in. (mm)

e_i = eccentricity of bar i with respect to centroid, in. (mm)

E_c = modulus of elasticity of concrete $= w_c^{1.5}\sqrt{f_c'}$ ksi $(= 5000\sqrt{f_c'}$, MPa)

E_s = modulus of elasticity of steel, which shall be taken as 29,000 ksi (210 MPa)

EI_{eff} = effective stiffness of composite section, kip-in.^{2} (N-mm^2)

f_c' = specified minimum concrete compressive strength, ksi (MPa)

F_y = yield strength of steel section, ksi (MPa)

F_{yr} = specified minimum yield strength of reinforcing bars, ksi (MPa)

h_1 = depth of the section

h_2 = width of the section

I_c = moment of inertia of the concrete section, in.^{4} (mm^4)

I_s = moment of inertia of steel shape, in.^{4} (mm^4)

I_{sr} = moment of inertia of reinforcing bars, in.^{4} (mm^4)

K = effective length factor determined in accordance with Chapter C

L = laterally unbraced length of the member, in. (mm)

N = number of longitudinal reinforcing bars

t_f = flange thickness, in. (mm)

t_w = depth of steel section, in. (mm)

w_c = weight of concrete per unit volume ($90 \le w_c \le 150$, lb/ft^3 or $1{,}440 \le w_c \le 2{,}450$, kg/m^3)

REFERENCES

ACI (2005), *Building Code Requirements for Structural Concrete*, ACI 318-05, American Concrete Institute, Farmington Hills, MI.

AISC (1999), *Load and Resistance Factor Design Specification for Structural Steel Buildings*, American Institute of Steel Construction, Chicago, IL.

AISC (2001), *LRFD Manual of Steel Construction*, 3rd Edition, American Institute of Steel Construction, Chicago, IL.

AISC (2005a), *Specification for Structural Steel Buildings*, ANSI/AISC 360-05, American Institute of Steel Construction, Chicago, IL.

AISC (2005b), *Steel Construction Manual*, 13th Edition, American Institute of Steel Construction, Chicago, IL.

Kim, D.K. (2005), "A Database for Composite Columns," M.S. Thesis, School of Civil and Environmental Engineering, Georgia Institute of Technology, Atlanta, GA.

Leon, R.T., Kim, D.K., and Hajjar, J.F. (2007), "Limit State Response of Composite Columns and Beam-Columns: Formulation of Design Provisions for the 2005 AISC Specification," *Engineering Journal*, AISC, No. 4, 4th Quarter, pp. 341–358.

Roik, K. and Bergmann, R. (1992),. "Composite Columns," in *Constructional Steel Design*, Dowling, P., Harding, J.E. and Bjorhovde, R. (eds.), Elsevier Science Publishers, New York, pp. 443–470.

Viest, I.M., Colaco, J.P., Furlong, R.W., Griffis, L.G., Leon, R.T., and Wyllie, L.A., Jr. (1997), *Composite Construction: Design for Buildings*, McGraw-Hill, New York, NY.

TABLE 1 - STRESS DISTRIBUTIONS FOR ANCHOR POINTS IN THE INTERACTION CURVE

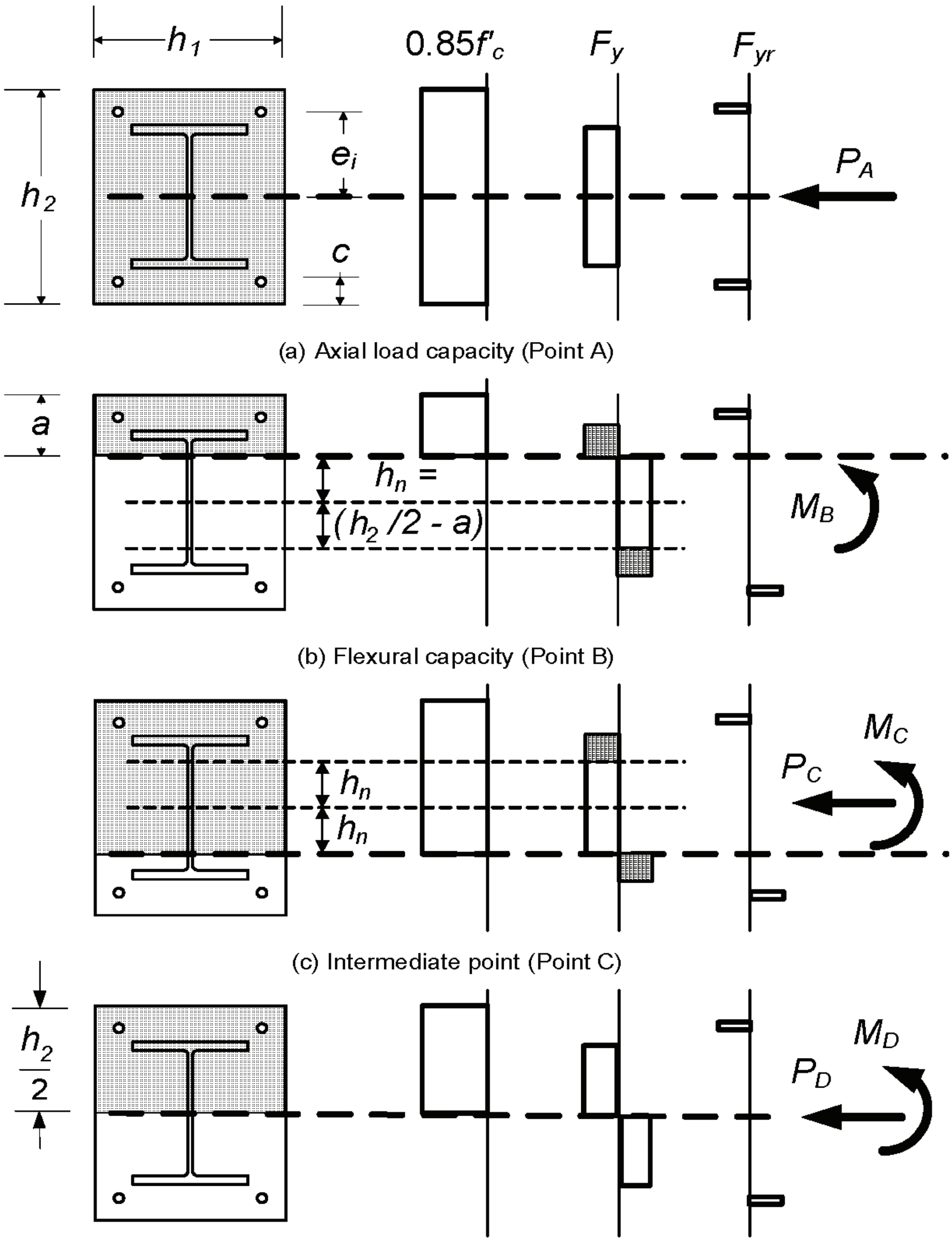

(a) Axial load capacity (Point A)

(b) Flexural capacity (Point B)

(c) Intermediate point (Point C)

(d) Balance point (Point D)

TABLE 2 - PLASTIC CAPACITIES FOR RECTANGULAR,ENCASED W-SHAPES BENT ABOUT THE X-X AXIS

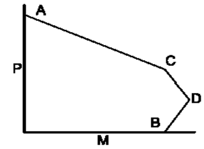

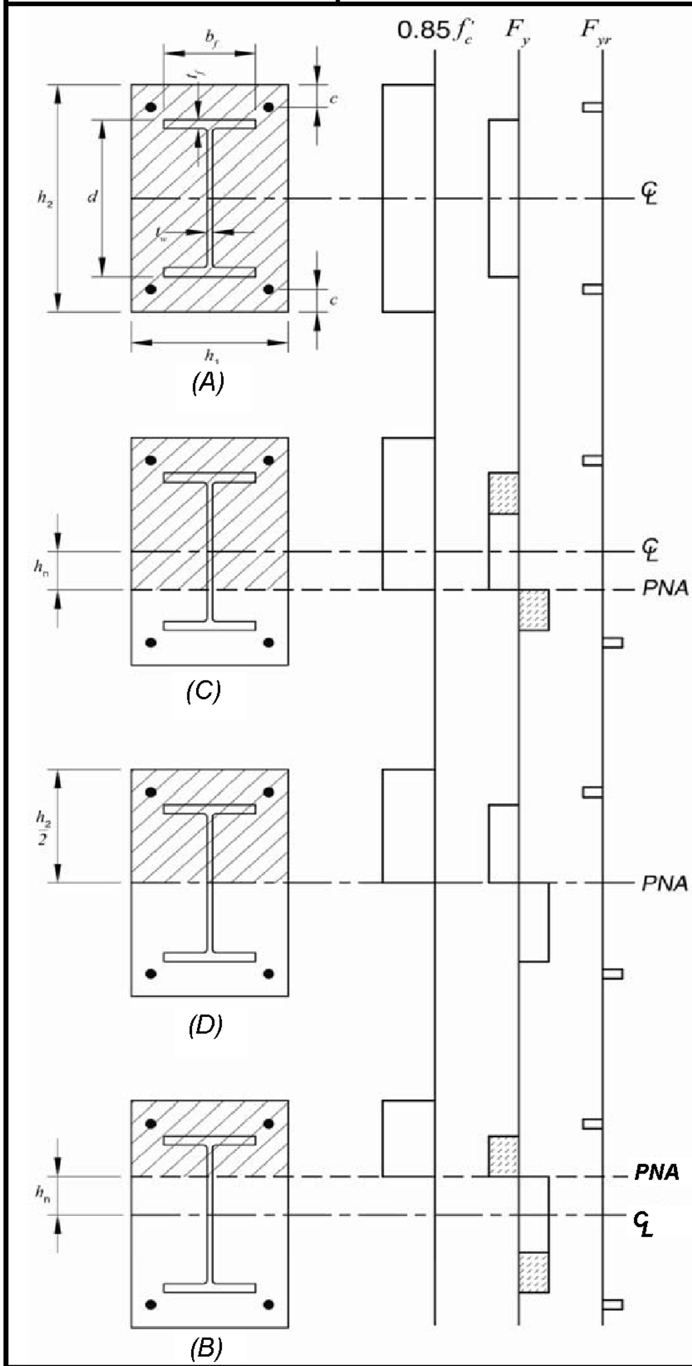

Section	Stress Distribution	Point	Defining Equations
(A)		A	$P_A = A_s F_y + A_{sr} F_{yr} + 0.85 f_c' A_c$ $M_A = 0$ A_s = area of steel shape A_{sr} = area of continuous reinforcing bars $A_c = h_1 h_2 - A_s - A_{sr}$
(C)		C	$P_C = 0.85 f_c' A_c$ $M_C = M_B$
		D	$P_D = \dfrac{0.85 f_c' A_c}{2}$ $M_D = Z_s F_y + Z_r F_{yr} + \tfrac{1}{2} Z_c \left(0.85 f_c'\right)$ $Z_r = A_{sr}\left(\dfrac{h_2}{2} - c\right) \qquad Z_s = b_f t_f \left(d - t_f\right) + \dfrac{\left(d - 2t_f\right)^2 t_w}{4}$ $Z_c = \dfrac{h_1 h_2^2}{4} - Z_s - Z_r$
(D)			
(B)		B	$P_B = 0$ $M_B = M_D - Z_{sn} F_y - \tfrac{1}{2} Z_{cn} \left(0.85 f_c'\right)$ $Z_{cn} = h_1 h_n^2 - Z_{sn} \qquad Z_{sn} = t_w h_n^2$ For h_n below the flange $\left(h_n < \dfrac{d}{2} - t_f\right)$: $h_n = \dfrac{0.85 f_c' A_c}{2\left[0.85 f_c' \left(h_1 - t_w\right) + 2 t_w F_y\right]}$ For h_n within the flange $\left(d/2 - t_f < h_n < d/2\right)$: $h_n = \dfrac{0.85 f_c' \left(A_c + A_s - d b_f\right) - 2F_y \left(A_s - d b_f\right)}{2\left[0.85 f_c' \left(h_1 - b_f\right) + 2F_y b_f\right]}$ $Z_{sn} = Z_s - b_f \left(d/2 - h_n\right)\left(d/2 + h_n\right)$ For h_n above the flange $\left(h_n > d/2\right)$: $h_n = \dfrac{0.85 f_c' \left(A_c + A_s\right) - 2F_y A_s}{2\left(0.85 f_c' h_1\right)}$ $Z_{sn} = Z_s = x$-axis plastic section modulus

TABLE 3 - PLASTIC CAPACITIES FOR RECTANGULAR, ENCASED W-SHAPES BENT ABOUT THE Y-Y AXIS

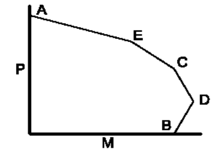

Section	Stress Distribution	Point	Defining Equations
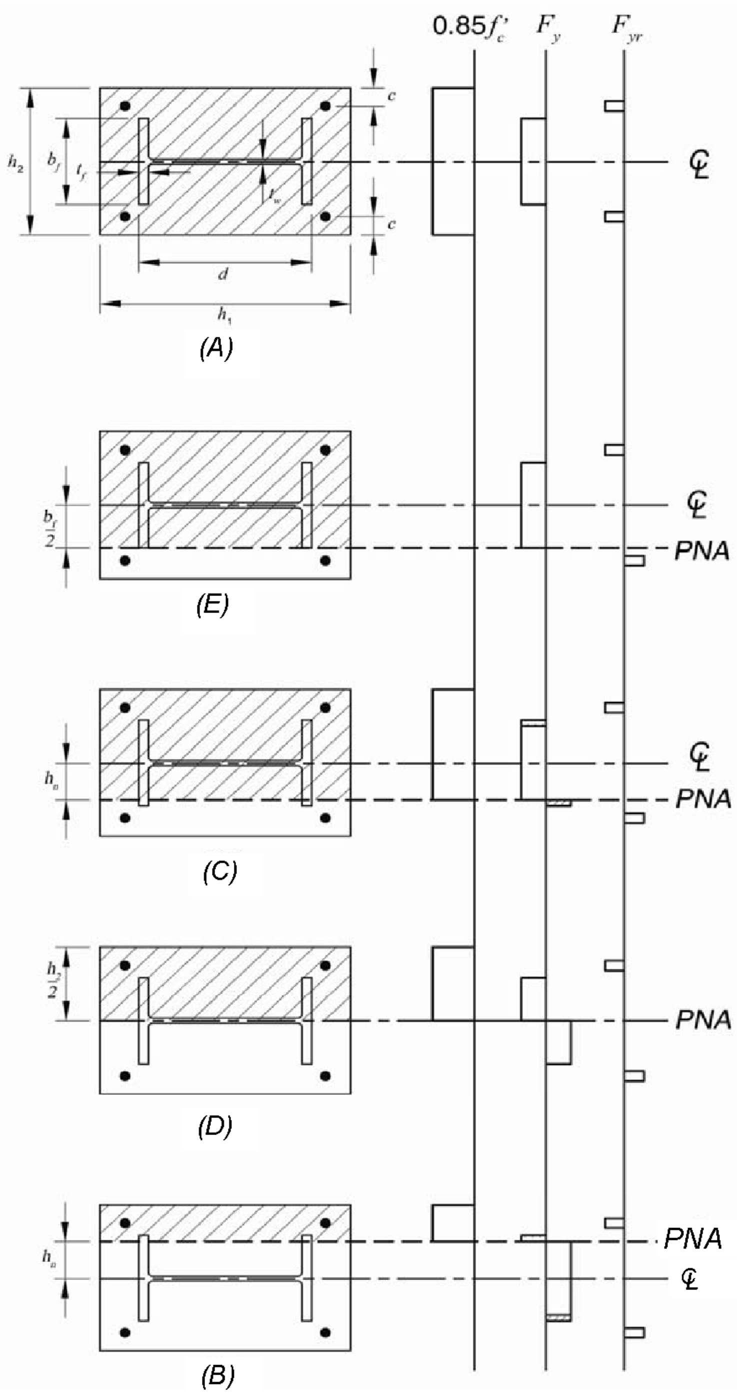		A	$P_A = A_s F_y + A_{sr} F_{yr} + 0.85 f_c' A_c \qquad M_A = 0$ A_s = area of steel shape A_{sr} = area of continuous reinforcing bars $A_c = h_1 h_2 - A_s - A_{sr}$
		E	$P_E = A_s F_y + (0.85 f_c')\left[A_c - \frac{h_1}{2}(h_2 - b_f) + \frac{A_{sr}}{2}\right]$ $M_E = M_D - Z_{sE} F_y - \frac{1}{2} Z_{cE}(0.85 f_c')$ $Z_{sE} = Z_{sy} = y$-axis plastic section modulus $Z_{cE} = \frac{h_1 b_f^2}{4} - Z_{sE}$
		C	$P_C = 0.85 f_c' A_c$ $M_C = M_B$
		D	$P_D = \frac{0.85 f_c' A_c}{2}$ $M_D = Z_s F_y + Z_r F_{sr} + \frac{1}{2} Z_c (0.85 f_c')$ Z_s = full y-axis plastic section modulus $Z_r = A_{sr}\left(\frac{h_2}{2} - c\right) \qquad Z_s = \frac{t_f b_f^2}{2} + \frac{(d - 2t_f) t_w^2}{4}$ $Z_c = \frac{h_1 h_2^2}{4} - Z_s - Z_r$
		B	$M_B = M_{\Delta} - Z_{sn} F_y - \frac{1}{2} Z_{cn} (0.85 f_c') \qquad P_B = 0$ $Z_{cn} = h_1 h_n^2 - Z_{sn}$ For h_n below the flange $\left(\frac{t_w}{2} < h_n < \frac{b_f}{2}\right)$: $h_n = \frac{0.85 f_c' (A_c + A_s - 2 t_f b_f) - 2F_y (A_s - 2 t_f b_f)}{2\left[4 t_f F_y + 0.85 f_c' (h_1 - 2 t_f)\right]}$ For h_n above the flange $\left(h_n > \frac{b_f}{2}\right)$: $h_n = \frac{0.85 f_c' (A_c + A_s) - 2 F_y A_s}{2\left[0.85 f_c' h_1\right]}$ $Z_{sn} = Z_{sy} = y$-axis plastic section modulus

TABLE 4 - PLASTIC CAPACITIES FOR COMPOSITE, FILLED HSS BENT ABOUT THE X-X AXIS

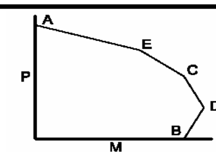

Section	Stress Distribution

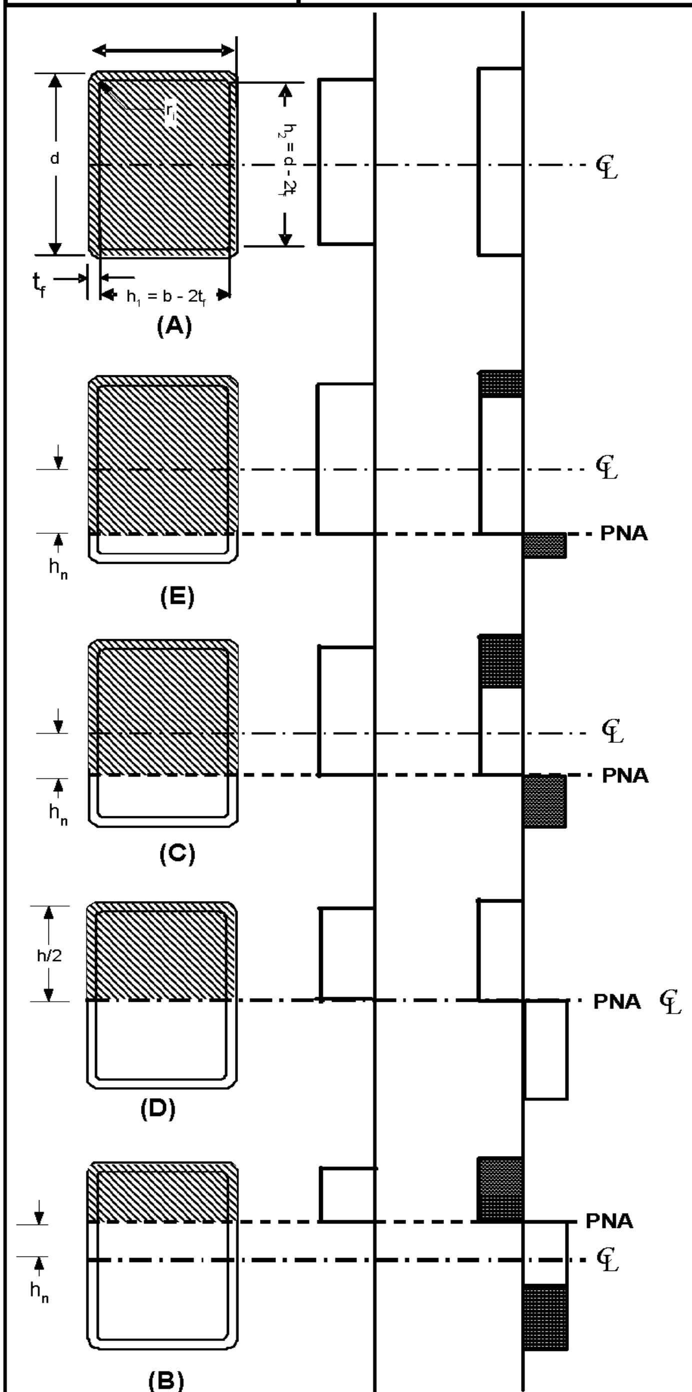

Point	Defining Equations
A	$P_A = A_s F_y + A_c\left(0.85 f_c'\right)$ $M_A = 0$ A_s = area of steel shape $A_c = h_1 h_2 - 0.858 r_i^2$ $h_1 = b - 2t_f$ $h_2 = d - 2t_f$
E	$P_E = \frac{1}{2}(0.85 f_c')A_c + 0.85 f_c' h_1 h_E + 4 F_y t_w h_E$ $M_E = M_{max} - \Delta M_E$ $Z_{sE} = b h_E^2 - Z_{cE}$ $\quad Z_{cE} = h_1 h_E^2$ $\Delta M_E = Z_{sE} F_y + ½ Z_{cE}\left(0.85 f_c'\right)$ $h_E = \frac{h_n}{2} + \frac{d}{4}$
C	$P_C = A_c\left(0.85 f_c'\right)$ $M_C = M_B$
D	$P_D = \frac{0.85 f_c' A_c}{2}$ $M_D = Z_s F_y + ½ Z_c\left(0.85 f_c'\right)$ Z_s = full y-axis plastic section modulus of steel shape $Z_c = \frac{h_1 h_2^2}{4} - 0.192 r_i^3$
B	$P_B = 0$ $M_B = M_D - Z_{sn} F_y - ½ Z_{cn}\left(0.85 f_c'\right)$ $Z_{sn} = 2 t_w h_n^2$ $Z_{cn} = h_1 h_n^2$ $h_n = \frac{0.85 f_c' A_c}{2\left[0.85 f_c' h_1 + 4 t_w F_y\right]} \le \frac{h_2}{2}$

TABLE 5 - PLASTIC CAPACITIES FOR COMPOSITE, FILLED ROUND HSS BENT ABOUT ANY AXIS

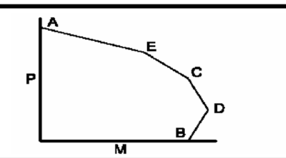

Section	Stress Distribution	Point	Defining Equations
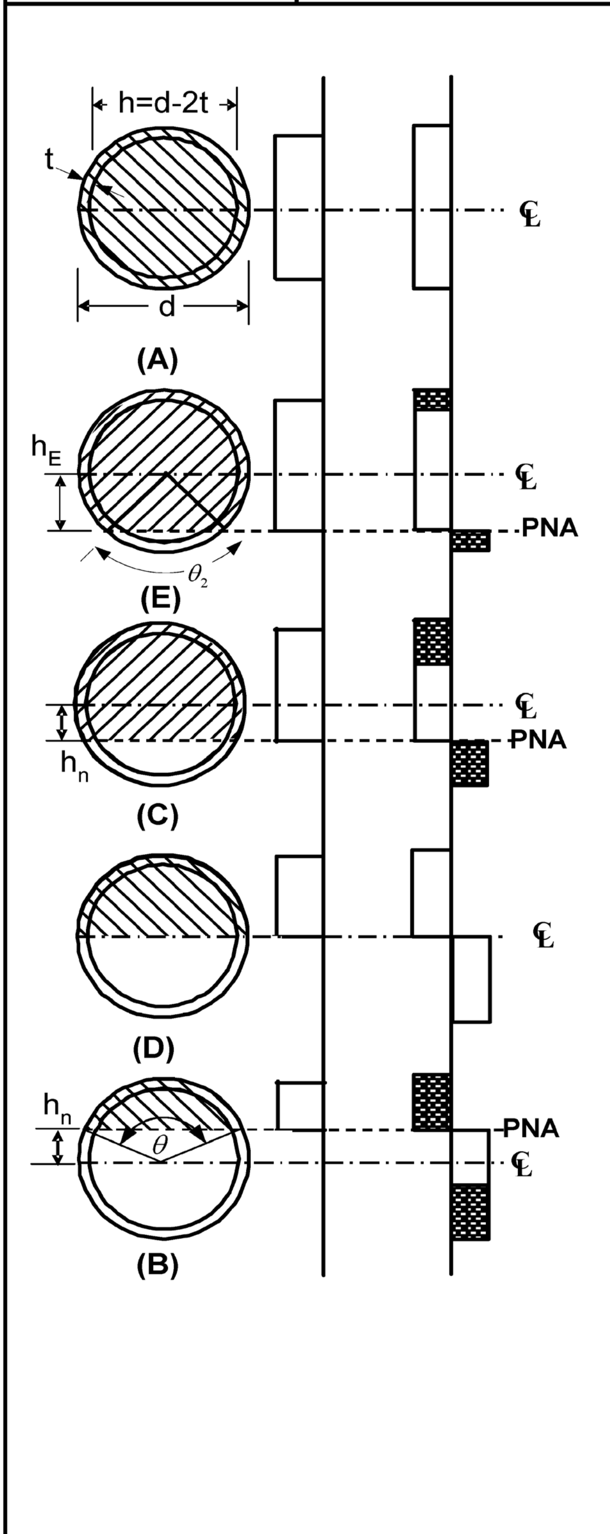		A	$P_A = A_s F_y + 0.95 f'_c A_c$ * $M_A = 0$ $A_s = 2\pi r_m t$ $r_m = \frac{d - t}{2}$ $A_c = \frac{\pi h^2}{4}$ * 0.95 instead of 0.85 can be used for the coefficient on the concrete compressive stress for all cases
		E	$h_E = \frac{h_n}{2} + \frac{h}{4}$ (h_n from Point B) $\theta_2 = \pi - 2\arcsin\left(\frac{2h_E}{h}\right)$ $Z_{sE} = \frac{d^3 - h^3}{6}\sin^3\left(\frac{\theta_2}{2}\right)X$ $X = \left[\frac{\theta_2}{\theta_2 - \sin\theta_2} + \frac{(2\pi - \theta_2)}{(2\pi - \theta_2) - \sin(2\pi - \theta_2)}\right]$ $Z_{sE} \approx \frac{d^3 - h^3}{6}\sin^{(4/3)}\left(\frac{\theta_2}{2}\right)$ $Z_{cE} = \frac{h^3}{6}\sin^3\left(\frac{\theta_2}{2}\right)$ $M_E = Z_{sE}F_y + \frac{1}{2}Z_{cE}\left(0.95 f'_c\right)$ $P_E = \left(0.95 f'_c A_c + F_y A_s\right) - \frac{1}{2}\left[F_y\left(d^2 - h^2\right) + \frac{1}{2}\left(0.95 f'_c\right) h^2\right]\left[\theta_2 - \sin\theta_2\right]$
		C	$P_C = 0.95 f'_c A_c$ $M_C = M_B$
		D	$P_D = \frac{0.95 f'_c A_c}{2}$ $M_D = Z_s F_y + ½ Z_c \left(0.95 f'_c\right)$ Z_s = plastic section modulus of steel shape = $\frac{d^3}{6} - Z_c$ $Z_c = \frac{h^3}{6}$
		B	$P_B = 0$ $M_B = Z_{sB}F_y + \frac{Z_{cB}\left(0.95 f'_c\right)}{2}$ $Z_{cB} = \frac{h^3 \sin^3(\theta/2)}{6}$ $Z_{sB} = \frac{d^3 - h^3}{12}\sin^3(\theta/2)\left[\frac{\theta}{\theta - \sin\theta} + \frac{(2\pi - \theta)}{(2\pi - \theta) - \sin(2\pi - \theta)}\right]$ $Z_{sB} \approx \frac{d^3 - h^3}{6}\sin^{(4/3)}(\theta/2)$ $\theta = \frac{0.0260K_c - 2K_s}{0.0848K_c} + \frac{\sqrt{\left(0.0260K_c + 2K_s\right)^2 + 0.857K_cK_s}}{0.0848K_c}$ $K_c = f'_c h^2$ $K_s = F_y\ r_m\ t$ $h_n = \frac{h}{2}\sin\left(\frac{\pi - \theta}{2}\right)$ (to be used in computing values for Point E)

DISCUSSION

Limit State Response of Composite Columns and Beam-Columns Part II: Application of Design Provisions for the 2005 AISC Specification

Paper by ROBERTO T. LEON and JEROME F. HAJJAR
(First Quarter, 2008)

Discussion by LOUIS F. GESCHWINDNER

The authors discuss the application of a set of equations for analysis and design of composite columns subjected to combined compression and bending. These equations were presented in the CD that accompanied the 13th edition *Steel Construction Manual* (AISC, 2005). The CD presents, in Figures I-1a through I-1d, sets of equations to be used to determine specific points on a simplified interaction diagram for encased W-shapes with bending about either the strong or the weak axes and filled rectangular and round HSS. These figures are used as the basis for Tables 2 through 5 in the paper. However, the authors have altered the figures from the CD for presentation in their paper.

The most significant difference between the authors' tables and the AISC figures occurs for the round HSS. The authors correctly point out a typographical error in Figure I-1d in the equation for θ where the terms $f'_c A_c$ should be removed. Clearly, if these variables were included in a calculation, the units, as well as the value, would be incorrect. The authors also point to "a discrepancy in the computation of Z_{sB}." However, the two equations that the authors provided for the plastic section modulus of the steel, Z_{sB}, appear to contain approximations that can be replaced with simple derivations that provide better accuracy. The paper does not include derivations for these equations.

In this discussion, three equations for use in determining Z_{sB} are developed and compared to those of the authors. The first equation is developed using the segment of a circle; the second, considered as a usable lower bound representation, is developed using the sector of a circle; and the third solution is developed as an exact solution.

Figure 1 shows the geometry of a concrete-filled round HSS. The plastic neutral axis is shown in the location that would result if the member were to undergo pure bending. This is point B in Table 5 of the paper and this figure is similar to that shown for point B in Table 5. The development of the flexural strength of the composite member requires the determination of several different properties of portions of the steel and concrete. One is the plastic section modulus, Z_{sB}, of that portion of the steel beyond the plastic neutral axis on the compression side and the symmetrically placed steel section on the tension side. These areas are shown shaded in Figure 1. The different solutions for Z_{sB} result from different approaches to modeling these two areas.

CIRCULAR SEGMENT

Figure 2(a) shows the geometric properties of a circular segment. Using these properties, the moment of the area of this circular segment taken about the circle center is

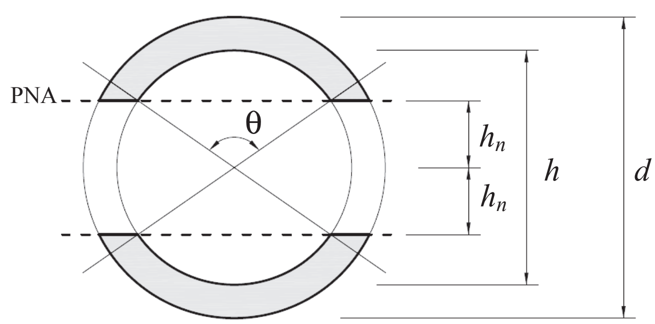

Fig. 1. Plastic neutral axis of concrete-filled round HSS in pure bending.

Louis F. Geschwindner, P.E., Ph.D., Vice President, American Institute of Steel Construction, 1 E. Wacker Dr., Suite 700, Chicago, IL 60601. E-mail: lfg@psu.edu

$$(\text{area})(\text{arm}) = \frac{r^2}{2}(\theta - \sin\theta)\left(\frac{4r}{3}\right)\left(\frac{\sin^3(\theta/2)}{(\theta - \sin\theta)}\right) = \left(\frac{2r^3}{3}\right)\sin^3(\theta/2) \tag{1}$$

Using $R = d/2$, the plastic section modulus for the pair of circular segments in tension and compression is twice the moment of the area of one circular segment. Thus,

$$Z_{seg} = 2\left(\frac{2(d/2)^3}{3}\right)\sin^3(\theta/2) = \frac{d^3}{6}\sin^3(\theta/2) \tag{2}$$

Similarly, the plastic section modulus for the matching segments of concrete with diameter, h, is

$$Z_{cB} = \frac{h^3}{6}\sin^3(\theta/2) \tag{3}$$

The plastic section modulus of the steel areas shown shaded in Figure 1, Z_{sB}, can then be determined as the plastic section modulus of the segment minus the plastic section modulus of the concrete. Thus,

$$Z_{sB} = Z_{seg} - Z_{cB} = \frac{(d^3 - h^3)}{6}\sin^3(\theta/2) \tag{4}$$

Equation 4 is the equation given in AISC Figure I-1d. This is not an exact solution since the two circle segments are not properly aligned. Figure 3 shows the areas that are used to determine Z_{seg} and Z_{cB} and where they are located with respect to each other. It also shows the area of steel that should have been included but is not, $A_{s,\text{missing}}$, and the area of concrete that was subtracted that should not have been, $A_{c,\text{extra}}$. As the thickness of the steel section gets smaller or the angle, θ, approaches π, Equation 4 approaches the correct value.

CIRCULAR SECTOR

Figure 2(b) shows the geometric properties of a circular sector. The moment of the area of the circular sector about the circle center is

$$(\text{area})(\text{arm}) = r^2\left(\frac{\theta}{2}\right)\left(\frac{2r\sin(\theta/2)}{3(\theta/2)}\right) = \frac{2}{3}r^3\sin(\theta/2) \tag{5}$$

Using $r = d/2$, the plastic section modulus for the pair of circular sectors in tension and compression is twice the moment of the area of one circular sector. Thus,

$$Z_{sec} = \frac{d^3}{6}\sin(\theta/2) \tag{6}$$

Similarly, the plastic section modulus for the matching sectors of concrete with diameter, h, is

$$Z_{conc} = \frac{h^3}{6}\sin(\theta/2) \tag{7}$$

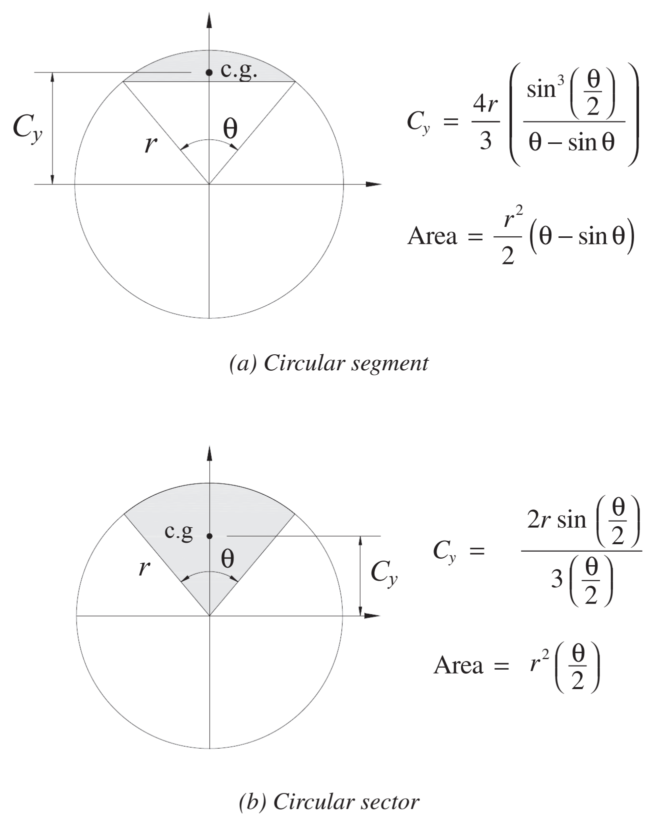

Fig. 2. Properties of a circle.

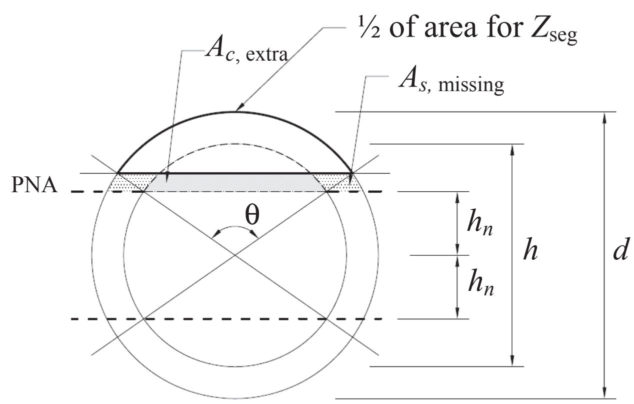

Fig. 3. Geometry for circular segment solution.

Subtracting the Z_{conc} from Z_{sec} will give the plastic section modulus of the steel. Thus,

$$Z_{sB} = \frac{\left(d^3 - h^3\right)}{6}\sin\left(\theta/2\right) \tag{8}$$

As was the case with the derivation of Equation 4, this is not an exact solution. Figure 4 shows the areas that are used to determine Z_{sec} and Z_{conc}. It also shows the area of steel that has not been included in the final calculation for Z_{sB}. Since the only approximation included in this derivation is the steel that has been ignored, this approach can be considered a "lower bound" solution.

EXACT SOLUTION

An exact solution is possible using the geometry of the circular segment and properly accounting for the two angles needed to describe the steel and concrete geometry. Figure 5(a) shows the concrete-filled round HSS with two circular segments defined by the angles, θ and θ_s. The angle, θ, is the same angle as defined for the earlier two derivations. The angle, θ_s, is the angle that defines the location of the plastic neutral axis at the outer face of the steel. Using the plastic section modulus as defined by Equation 2 and θ_s, yields

$$Z_{seg} = \frac{d^3}{6}\sin^3\left(\theta_s/2\right) \tag{9}$$

For the concrete segment, using Equation 2 and θ, yields

$$Z_{cB} = \frac{h^3}{6}\sin^3\left(\theta/2\right) \tag{10}$$

The exact plastic section modulus for the steel is then

$$Z_{sB} = Z_{seg} - Z_{cB} \tag{11}$$

In order to combine Equations 9 and 10, the relationship between θ and θ_s is needed. From Figure 5(b), the following relationship is seen

$$\frac{h}{2}\cos\left(\theta/2\right) = \frac{d}{2}\cos\left(\theta_s/2\right) \tag{12}$$

and combined with the basic trigonometric relationship, $\sin A = \sqrt{1-\cos^2 A}$, yields

$$\sin\left(\theta_s/2\right) = \left(1 - \frac{h^2}{d^2}\cos^2\left(\theta/2\right)\right)^{1/2} \tag{13}$$

Substituting Equation 13 into Equation 9 yields

$$Z_{seg} = \frac{d^3}{6}\left(1 - \frac{h^2}{d^2}\cos^2\left(\theta/2\right)\right)^{3/2} \tag{14}$$

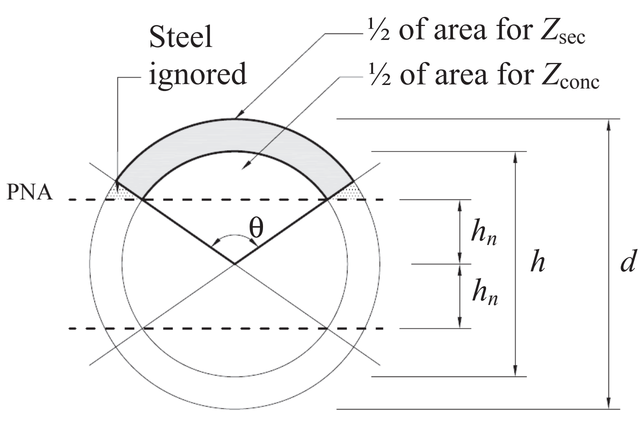

Fig. 4. Geometry for circular sector solution.

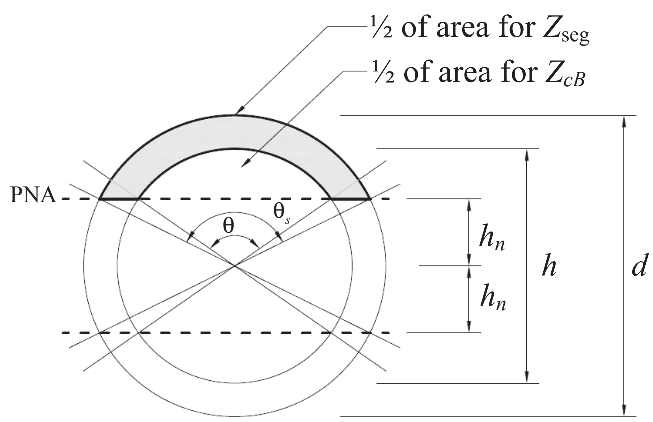

(a) Geometry

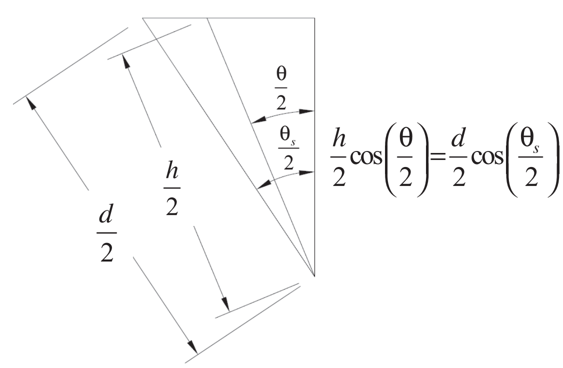

(b) Relationship between θ and θ_s

Fig. 5. Geometry for exact solution.

and substituting Equations 10 and 14 into Equation 11 yields

$$Z_{sB} = \frac{d^3}{6}\left(1 - \frac{h^2}{d^2}\cos^2\left(\theta/2\right)\right)^{3/2} - \frac{h^3}{6}\sin^3\left(\theta/2\right) \tag{15}$$

Unlike the two previous derivations given for the circular segment and the circular sector, this derivation gives the exact solution for Z_{sB}.

AUTHORS' EQUATIONS

The two equations presented in the paper for Z_{sB} are:

a "correct" formulation

$$Z_{sB} = \left(\frac{d^3 - h^3}{12}\right)\sin^3\left(\theta/2\right) \times \left[\frac{\theta}{\theta - \sin\theta} + \frac{\left(2\pi - \theta\right)}{\left(2\pi - \theta\right) - \sin\left(2\pi - \theta\right)}\right] \tag{16}$$

and a simplified approximation

$$Z_{sB} \approx \frac{\left(d^3 - h^3\right)}{6}\sin^{4/3}\left(\theta/2\right) \tag{17}$$

COMPARISON OF RESULTS

Five equations for the plastic section modulus of the steel for point B, pure bending, of a concrete-filled round HSS have been presented. The results from these five equations are plotted in Figure 6 for an HSS 16.000×0.250 over the full range of angle, θ, from 0 to π.

Equation 4, the original AISC equation, is the least accurate of the equations derived in this discussion. Equation 8, the "lower bound" solution is closer to the exact solution than all of the other equations shown. The two equations presented by the authors, Equations 16 and 17, appear to be unrelated to those derived in this discussion. Although they give values closer to the exact solution than Equation 4, they do not provide a better solution than Equation 8, the "lower bound" solution. The origins of Equations 16 and 17 are not discussed in the paper.

The difference between Equations 8 and 15 is greatest for the lower values of θ. Thus, it would be helpful to know the approximate range of θ for realistic round HSS and acceptable values of concrete strengths. As concrete strength increases, the angle, θ, decreases. Thus, a check was made for all of the concrete filled round HSS listed in the Composite Column Tables of the 13th edition *Steel Construction Manual* (AISC, 2005b) but with a concrete strength, f'_c = 10.0 ksi. For these shapes, with F_y = 42 ksi, the HSS 16.000×0.250 required the smallest angle, θ = 1.77 rad. As seen in Figure 6 for this shape, Equations 4, 8, 15, 16 and 17 give the following values for Z_{sB}:

Eq. No.	Model	Z_{sB} (in.^{3})
4	Circular segment	26.9
8	Circular sector	44.8
15	Exact	45.3
16	Paper "correct"	41.1
17	Paper simplified	41.2

In addition to using the Z_{sB} equations for determining moment strength for the pure bending case, the same basic formulation is used by the authors, with θ_2 to determine Z_{sE}, for moment strength at point E. The realistic range for θ_2 is π to 0 as points between C and somewhere close to A are determined. Thus, the error in not using Equation 15 with

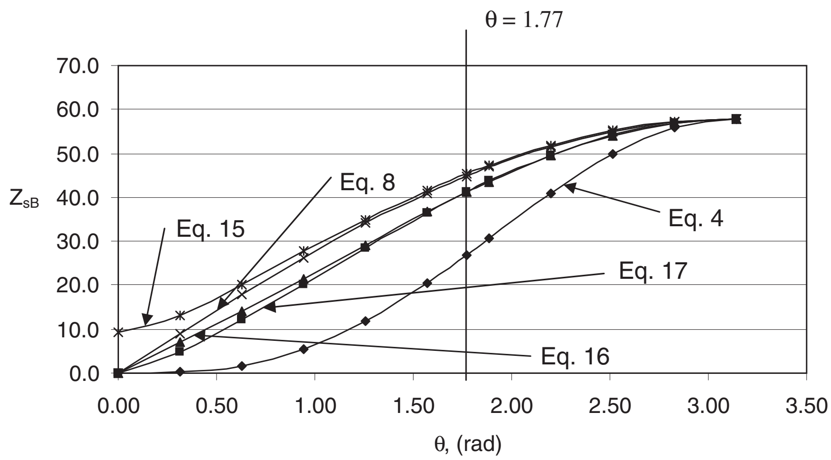

Fig. 6. Comparison of five equations for Z_{sB} for an HSS 16.000×0.250.

θ_2 for these points can be quite substantial. However, the lowest value of θ_2 for point E as defined by the authors for the HSS 16.000×0.250 discussed earlier is 1.23 rad and the error in computing Z_{sE} using the "lower bound" equation is approximately 5%.

RECOMMENDATIONS

Based on the derivations presented in this discussion, it is recommended that either the exact solution, Equation 15, or the circular sector solution, Equation 8, be used in calculations for pure bending, Point B, for a concrete-filled round HSS. Considering the simplicity of the latter and its ability to closely represent the correct value for Z_{sB}, it is further recommended that Equation 8 be adopted for use in place of the currently listed equation in Figure I-1d of the 13th edition companion CD.

In the rare case where point E is to be determined, it is recommended that the lower bound equation, Equation 8 with θ_2, be used. If more points on the interaction curve are to be determined, the exact solution, Equation 15, should be used.

In addition, revised versions of Figures I-1a through I-1d from the CD Companion V.13.0 are presented as Tables A through D of this Discussion. Note that Tables A through D also correspond to Figures 2 through 5 of the Leon and Hajjar paper, but with corrections.

In summary the revisions incorporated are:

1. No changes to Figure I-1a (Table A).
2. Two editorial changes in Figure I-1b (Table B).
3. Several editorial changes and the inclusion of equations for point E in Figure I-1c (Table C).
4. Several editorial changes, the inclusion of equations for point E, and updated equations for Z_{sB} and Z_{sE} in Figure I-1d (Table D).

REFERENCE

AISC (2005), *Steel Construction Manual,* 13th Edition, American Institute of Steel Construction, Chicago, IL.

Editor's Note: AISC's Committee on Manuals and Textbooks has decided to incorporate Dr. Geschwindner's recommendations in revisions that will be made with the 14th edition AISC Steel Construction Manual.

Table A.
Plastic Capacities for Rectangular, Encased W-Shapes Bent About the X-X Axis

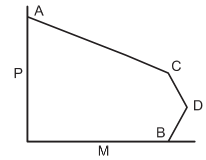

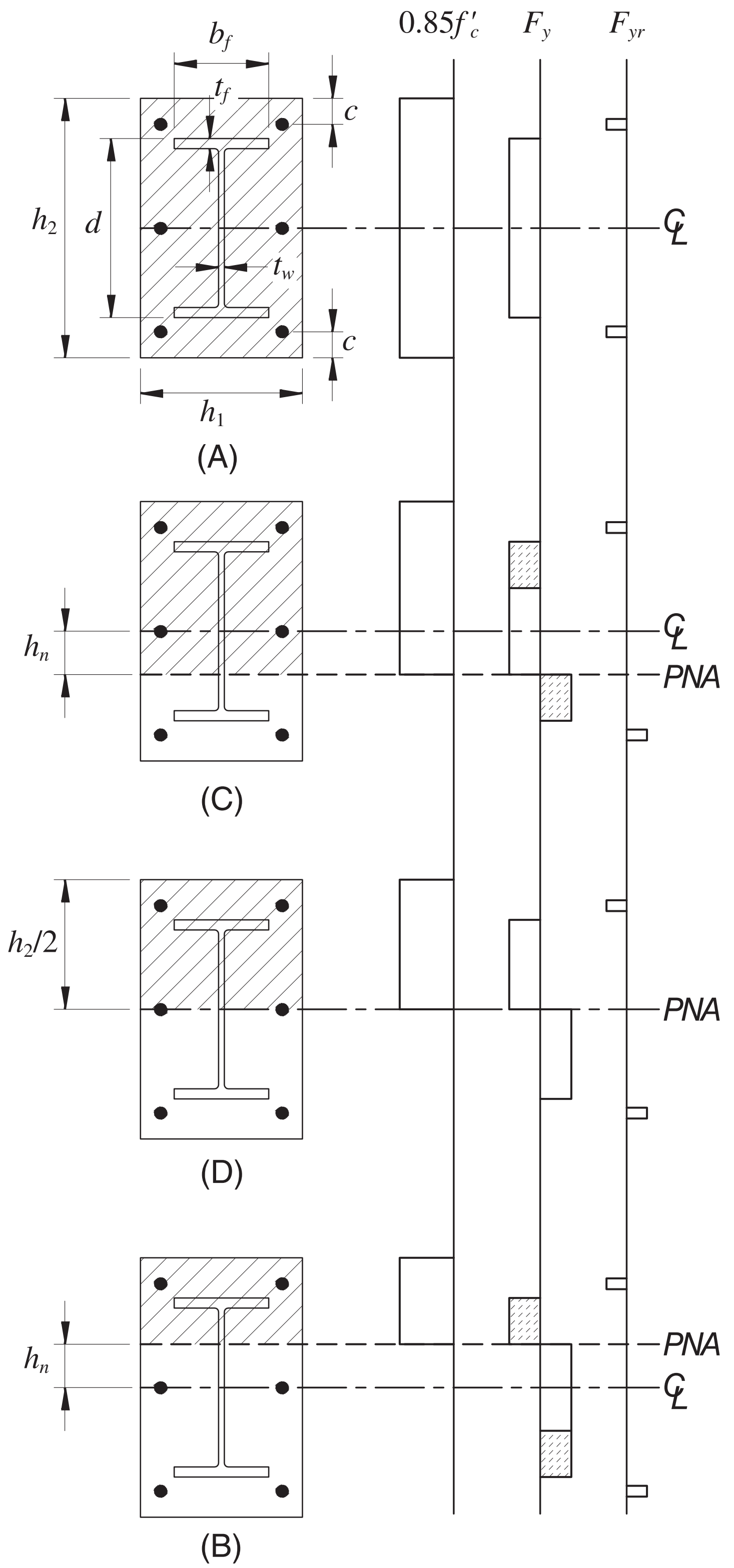

Section	Stress Distribution	Point	Defining Equations
		A	$P_A = A_s F_y + A_{sr} F_{yr} + 0.85 f'_c A_c$ $M_A = 0$ A_s = area of steel shape A_{sr} = area of all continuous reinforcing bars $A_c = h_1 h_2 - A_s - A_{sr}$
		C	$P_C = 0.85 f'_c A_c$ $M_C = M_B$
		D	$P_D = \frac{0.85 f'_c A_c}{2}$ $M_D = Z_s F_y + Z_r F_{yr} + \frac{Z_c}{2}(0.85 f'_c)$ Z_s = full x-axis plastic section modulus of steel shape A_{srs} = area of continuous reinforcing bars at the centerline $Z_r = (A_{sr} - A_{srs})\left(\frac{h_2}{2} - c\right)$ $Z_c = \frac{h_1 h_2^2}{4} - Z_s - Z_r$
		B	$P_B = 0$ $M_B = M_D - Z_{sn} F_y - \frac{1}{2} Z_{cn}(0.85 f'_c)$ $Z_{cn} = h_1 h_n^2 - Z_{sn}$ For h_n below the flange $\left(h_n \le \frac{d}{2} - t_f\right)$ $h_n = \frac{0.85 f'_c (A_c + A_{srs}) - 2F_{yr} A_{srs}}{2\left[0.85 f'_c (h_1 - t_w) + 2F_y t_w\right]}$ $Z_{sn} = t_w h_n^2$ For h_n within the flange $\left(\frac{d}{2} - t_f < h_n \le \frac{d}{2}\right)$ $h_n = \frac{0.85 f'_c \left(A_c + A_s - d b_f + A_{srs}\right) - 2F_y \left(A_s - d b_f\right) - 2F_{yr} A_{srs}}{2\left[0.85 f'_c \left(h_1 - b_f\right) + 2F_y b_f\right]}$ $Z_{sn} = Z_s - b_f \left(\frac{d}{2} - h_n\right)\left(\frac{d}{2} + h_n\right)$ For h_n above the flange $\left(d_n > \frac{d}{2}\right)$ $h_n = \frac{0.85 f'_c (A_c + A_s + A_{srs}) - 2F_y A_s - 2F_{yr} A_{srs}}{2(0.85 f'_c h_1)}$ $Z_{sn} = Z_{sx}$ = full x-axis plastic section modulus of steel shape

Table B.
Plastic Capacities for Rectangular, Encased W-Shapes Bent About the Y-Y Axis

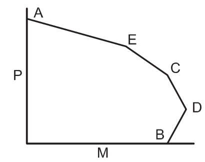

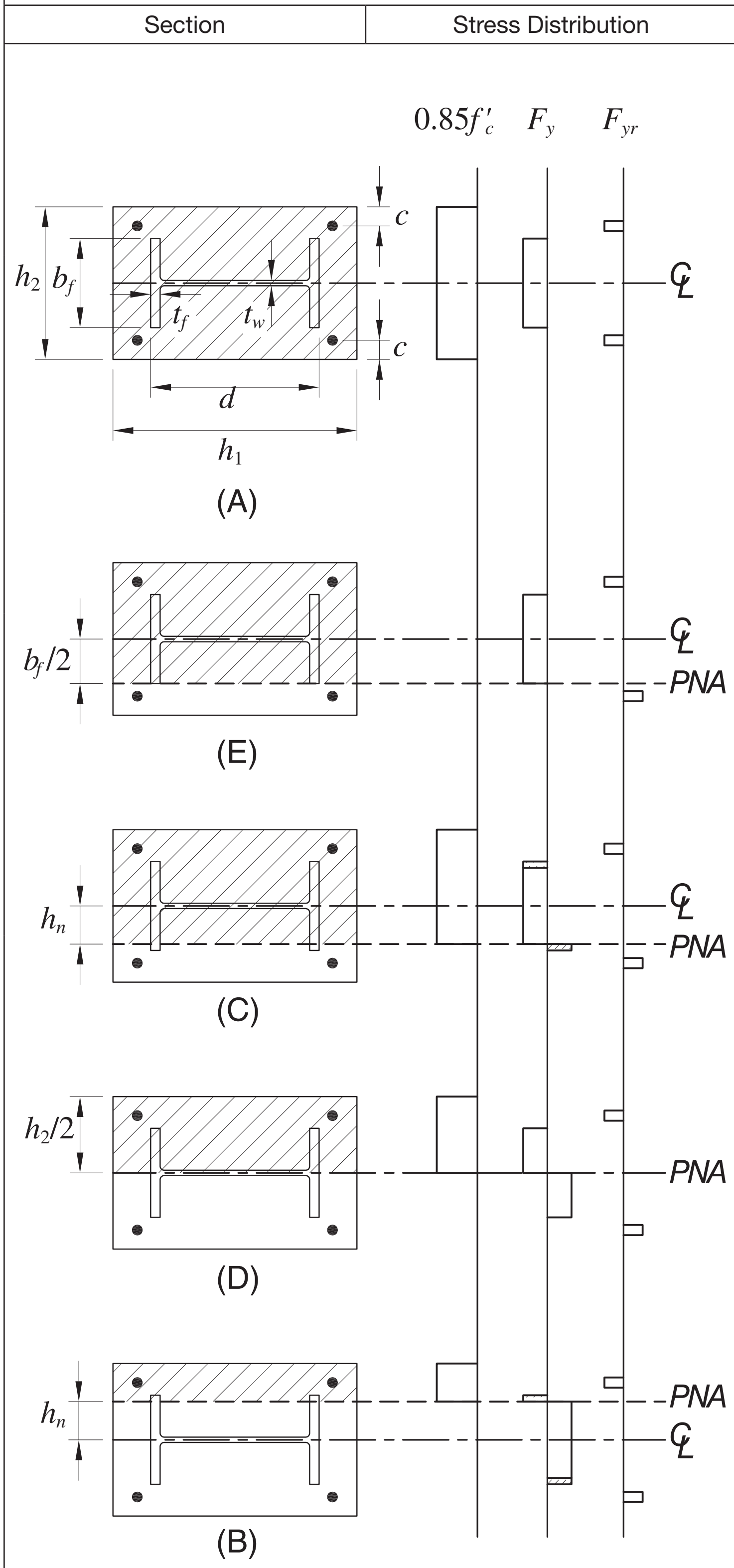

Point	Defining Equations
A	$P_A = A_sF_y + A_{sr}F_{yr} + 0.85f'_cA_c$ $M_A = 0$ A_s = area of steel shape A_{sr} = area of continuous reinforcing bars $A_c = h_1h_2 - A_s - A_{sr}$
E	$P_E = A_sF_y + (0.85f'_c)\left[A_c - \frac{h_1}{2}(h_2 - b_f) + \frac{A_{sr}}{2}\right]$ $M_E = M_D - Z_{sE}F_y - \frac{1}{2}Z_{cE}(0.85f'_c)$ $Z_{sE} = Z_{sy}$ = full y-axis plastic section modulus of steel shape $Z_{cE} = \frac{h_1b_f^2}{4} - Z_{sE}$
C	$P_C = 0.85f'_cA_c$ $M_C = M_B$
D	$P_D = \frac{0.85f'_cA_c}{2}$ $M_D = Z_sF_y + Z_rF_{sr} + \frac{1}{2}Z_c(0.85f'_c)$ Z_s = full y-axis plastic section modulus of steel shape $Z_r = A_{sr}\left(\frac{h_2}{2} - c\right)$ $Z_c = \frac{h_1h_2^2}{4} - Z_s - Z_r$
B	$P_B = 0$ $M_B = M_D - Z_{sn}F_y - \frac{1}{2}Z_{cn}(0.85f'_c)$ $Z_{cn} = h_1h_n^2 - Z_{sn}$ For h_n below the flange $\left(\frac{t_w}{2} < h_n \le \frac{b_f}{2}\right)$ $h_n = \frac{0.85f'_c(A_c + A_s - 2t_fb_f) - 2F_y(A_s - 2t_fb_f)}{2\left[4t_fF_y + (h_1 - 2t_f)0.85f'_c\right]}$ $Z_{sn} = Z_s - 2t_f\left(\frac{b_f}{2} + h_n\right)\left(\frac{b_f}{2} - h_n\right)$ For h_n above the flange $\left(h_n > \frac{b_f}{2}\right)$ $h_n = \frac{0.85f'_c(A_c + A_s) - 2F_yA_s}{2\left[0.85f'_ch_1\right]}$ $Z_{sn} = Z_{sy}$ = full y-axis plastic section modulus of steel shape

Table C.
Plastic Capacities for Composite, Filled HSS Bent About the X-X Axis

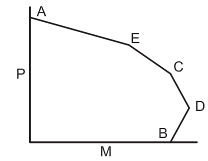

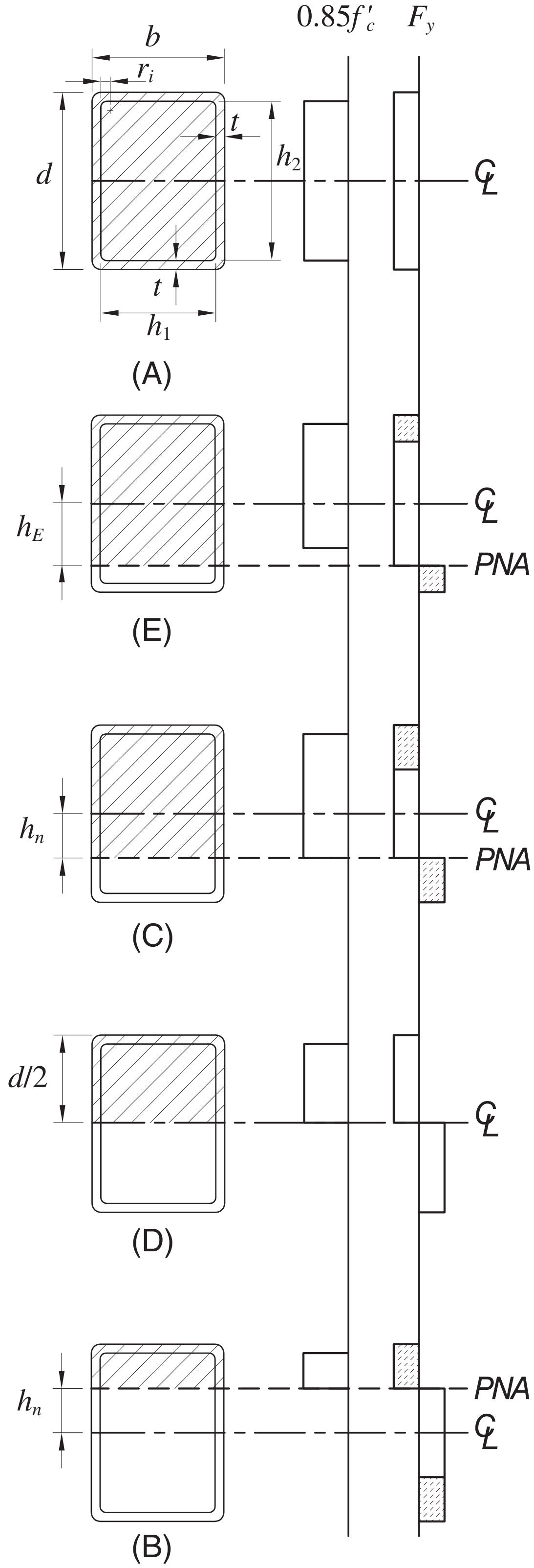

Section	Stress Distribution	Point	Defining Equations
(A)		A	$P_A = F_y A_s + 0.85 f'_c A_c$ $M_A = 0$ A_s = area of steel shape $A_c = h_1 h_2 - 0.858 r_i^2$ $h_1 = b - 2t$ $h_2 = d - 2t$
(E)		E	$P_E = \frac{1}{2}\left(0.85 f'_c A_c\right) + 0.85 f'_c h_1 h_E + 4 F_y t h_E$ $M_E = M_D - F_y Z_{sE} - \frac{1}{2}\left(0.85 f'_c Z_{cE}\right)$ $Z_{cE} = h_1 h_E^2$ $Z_{sE} = 2 t h_E^2$ $h_E = \frac{h_n}{2} + \frac{d}{4}$
(C)		C	$P_C = 0.85 f'_c A_c$ $M_C = M_B$
(D)		D	$P_D = \frac{0.85 f'_c A_c}{2}$ $M_D = F_y Z_s + \frac{1}{2}\left(0.85 f'_c Z_c\right)$ Z_s = full x-axis plastic section modulus of HSS $Z_c = \frac{h_1 h_2^2}{4} - 0.192 r_i^3$
(B)		B	$P_B = 0$ $M_B = M_D - F_y Z_{sn} - \frac{1}{2}\left(0.85 f'_c Z_{cn}\right)$ $Z_{sn} = 2 t h_n^2$ $Z_{cn} = h_1 h_n^2$ $h_n = \frac{0.85 f'_c A_c}{2\left[0.85 f'_c h_1 + 4 t F_y\right]} \le \frac{h_2}{2}$

Table D.
Plastic Capacities for Composite, Filled Round HSS Bent About Any Axis

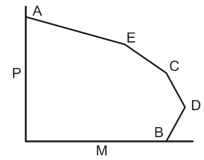

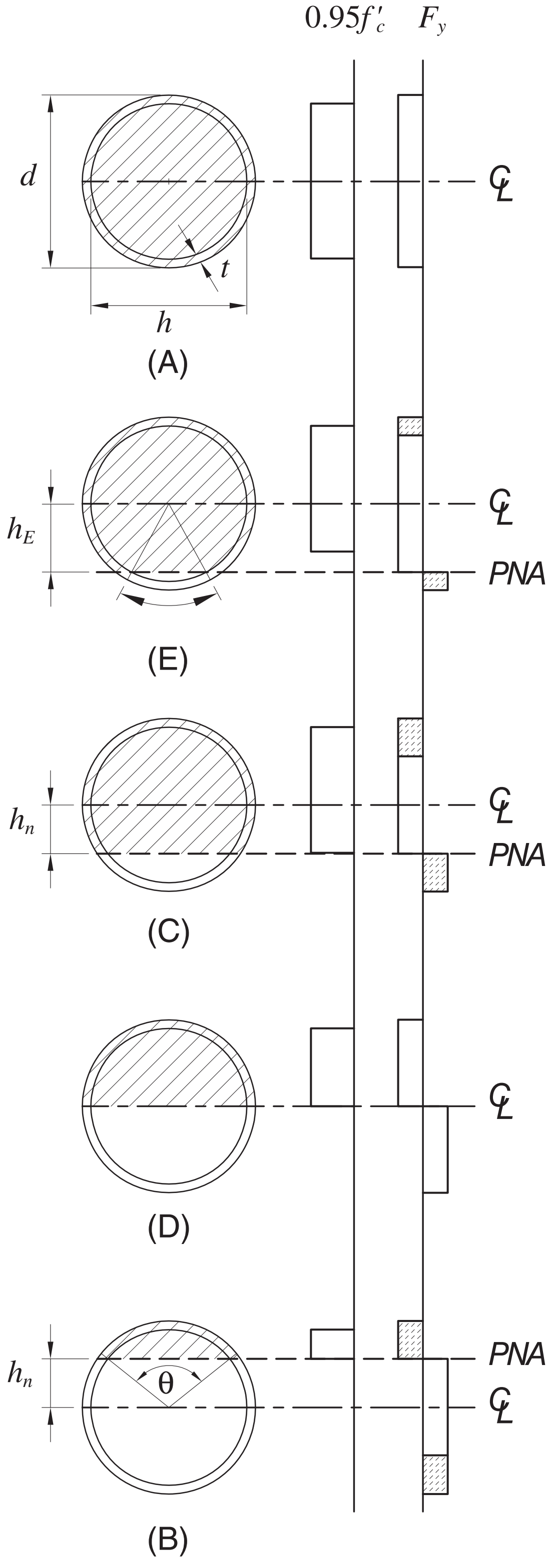

Section	Stress Distribution	Point	Defining Equations
(A)		A	$P_A = F_y A_s + 0.95 f'_c A_c$ * $M_A = 0$ $A_s = \pi(dt - t^2)$ $A_c = \dfrac{\pi h^2}{4}$
(E)		E	$P_E = P_A - \tfrac{1}{4}\left[F_y\left(d^2 - h^2\right) + \tfrac{1}{2}\left(0.95 f'_c\right)h^2\right]\left(\theta_2 - \sin\theta_2\right)$ $M_E = F_y Z_{sE} + \tfrac{1}{2}\left(0.95 f'_c Z_{cE}\right)$ $Z_{cE} = \dfrac{h^3}{6}\sin^3\left(\dfrac{\theta_2}{2}\right)$ $Z_{sE} = \dfrac{\left(d^3 - h^3\right)}{6}\sin\left(\dfrac{\theta_2}{2}\right)$ $h_E = \dfrac{h_n}{2} + \dfrac{h}{4}$ $\theta_2 = \pi - 2\arcsin\left(\dfrac{2h_E}{h}\right)$
(C)		C	$P_C = 0.95 f'_c A_c$ $M_C = M_B$
(D)		D	$P_D = \dfrac{0.95 f'_c A_c}{2}$ $M_D = F_y Z_s + \tfrac{1}{2}\left(0.95 f'_c Z_c\right)$ Z_s = plastic section modulus of steel shape $= \dfrac{d^3}{6} - Z_c$ $Z_c = \dfrac{h^3}{6}$
(B)		B	$P_B = 0$ $M_B = F_y Z_{sB} + \tfrac{1}{2}\left(0.95 f'_c Z_{cB}\right)$ $Z_{sB} = \dfrac{\left(d^3 - h^3\right)}{6}\sin\left(\dfrac{\theta}{2}\right)$ $Z_{cB} = \dfrac{h^3\sin^3\left(\dfrac{\theta}{2}\right)}{6}$ $\theta = \dfrac{0.0260K_c - 2K_s}{0.0848K_c} + \dfrac{\sqrt{\left(0.0260K_c + 2K_s\right)^2 + 0.857K_cK_s}}{0.0848K_c}$ (rad) $K_c = f'_c h^2$ $K_s = F_y\left(\dfrac{d-t}{2}\right)t$ ("thin" HSS wall assumed) $h_n = \dfrac{h}{2}\sin\left(\dfrac{\pi - \theta}{2}\right) \le \dfrac{h}{2}$

*$0.95f'_c$ may be used for concrete filled round HSS.

CLOSURE

Limit State Response of Composite Columns and Beam-Columns Part II: Application of Design Provisions for the 2005 AISC Specification

Paper by ROBERTO T. LEON and JEROME F. HAJJAR

Closure by ROBERTO T. LEON, TIZIANO PEREA and JEROME F. HAJJAR

The authors thank Dr. Geschwindner for his comments on the derivation of the plastic section modulus, Z_s, of circular HSS as shown in Table 5 of the original paper. (Equation numbers referenced in this Closure are the same as those used in the Discussion, for clarity.)

The derivation of Equation 16 of the Discussion was omitted from the original paper for brevity. It is shown in the attached Appendix. Equation 17 was intended as a straightforward lower-bound curve fit to Equation 16; many similar expressions are possible. The primary assumption that was made in Equation 16 is that the wall of the circular HSS is assumed to be thin (i.e., that $\theta \approx \theta_s$ using the nomenclature of the Discussion). As noted by Dr. Geschwindner, this assumption results in the area of the steel being underestimated and that for the concrete being overestimated.

The authors appreciate Dr. Geschwindner's efforts in developing new exact and approximate equations for Z_s, represented by Equations 15 and 8, respectively, in the Discussion. The authors agree that his equations are applicable to thick-walled circular CFTs ($\theta \neq \theta_s$) and provide results with better accuracy than those stated in the original paper.

The authors agree that Equation 8 in the Discussion is a reasonable replacement for both the original equation for Z_{sB} in Table I-1d on the CD companion to the 13th edition AISC *Manual* (Equation 4 in the Discussion) and the proposed equation for Z_{sB} in our original paper (Equation 17 in the Discussion). Finally, the authors will like to note that Equation 8 is the same as those given by the Architectural Institute of Japan (AIJ) in their provisions for composite members once a number of geometric transformations are made.

Roberto T. Leon, Professor, School of Civil and Environmental Engineering, 790 Atlantic Dr., Georgia Institute of Technology, Atlanta, GA 30332, corresponding author. E-mail: rl58@ce.gatech.edu

Tiziano Perea, Graduate Research Assistant, School of Civil and Environmental Engineering, 790 Atlantic Dr., Georgia Institute of Technology, Atlanta, GA 30332. E-mail: tperea@gatech.edu

Jerome F. Hajjar, Professor and Chair, Department of Civil and Environmental Engineering, 400 Snell Engineering Center, 360 Huntington Ave., Northeastern University, Boston, MA 02115. E-mail: jf.hajjar@neu.edu

APPENDIX

Derivation of the Plastic Section Modulus of a Circular HSS Thin Tube (Equation 16 in the Discussion)

This appendix derives the equation to get the plastic section modulus (Z_s) of a circular HSS stated in Table 5 in the original paper (Equation 15 in this appendix). The derivation assumes a thin-walled HSS cross section as shown in Figure A.1b.

The area and the centroidal distance of a circular segment (Figure A.1a) including both concrete and steel sections are given by:

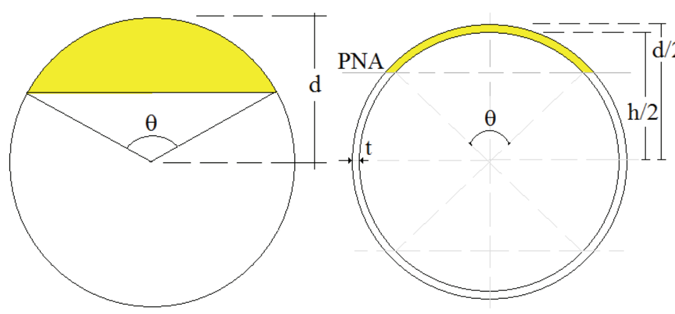

(a) Circular segment *(b) Circular HSS cross-section*

Fig. A.1. Variables used in the derivation.

$$A_d = \frac{d^2}{8}\left(\theta - \sin\theta\right) \tag{A.1}$$

$$Y_d = \frac{2d\sin^3\left(\theta/2\right)}{3\left(\theta - \sin\theta\right)} \tag{A.2}$$

Note in Figure A.1 that the angle θ in (a) is not the same as the angle θ in (b). This difference is small for thin-walled sections. Assuming the steel wall is thin enough that the difference can be neglected, the area and centroidal distance of the circular segment in the concrete only can be approximated as:

$$A_h = \frac{h^2}{8}\left(\theta - \sin\theta\right) \tag{A.3}$$

$$Y_h = \frac{2h\sin^3\left(\theta/2\right)}{3\left(\theta - \sin\theta\right)} \tag{A.4}$$

Thus, the area and the first moment of the area of the shaded ring segment in Figure A.1b are as follows:

$$A_r = A_d - A_h \tag{A.5}$$

$$Q_r = A_d Y_d - A_h Y_h \tag{A.6}$$

Then, the centroidal distance of a ring segment (i.e., only the steel) is given by:

$$Y_r = \frac{Q_r}{A_r} = \frac{2\left(d^3 - h^3\right)\sin^3\left(\theta/2\right)}{3\left(d^2 - h^2\right)\left(\theta - \sin\theta\right)} \tag{A.7}$$

The last equation can be adjusted for the complement ring segment when θ is changed by 2π – θ. Thus:

$$Y_r = \frac{Q_r}{A_r} = \frac{2\left(d^3 - h^3\right)\sin^3\left(\theta/2\right)}{3\left(d^2 - h^2\right)\left(2\pi - \theta + \sin\theta\right)} \tag{A.8}$$

The compression and tension forces on the steel ring segments, their respective centroidal distances, and the total bending moment are given by the following equations.

For the compression zone defined by the angle θ, where $r_m = (d - t)/2$ and $t = (d - h)/2$:

$$\begin{aligned} C_s &= 2\pi r_m t\left(\frac{\theta}{2\pi}\right)F_y = \left(\frac{d-t}{2}\right)(t)(\theta)F_y \\ &= \frac{\left(d^2 - h^2\right)(\theta)F_y}{8} \end{aligned} \tag{A.9}$$

$$Y_{cs} = \frac{2\left(d^3 - h^3\right)\sin^3\left(\theta/2\right)}{3\left(d^2 - h^2\right)\left(\theta - \sin\theta\right)} \tag{A.10}$$

For the tension zone defined by the complement of the angle θ, where $r_m = (d - t)/2$ and $t = (d - h)/2$:

$$T_s = \left(\frac{d-t}{2}\right)(t)\left(2\pi - \theta\right)F_y = \frac{\left(d^2 - h^2\right)\left(2\pi - \theta\right)F_y}{8} \tag{A.11}$$

$$Y_{ts} = \frac{2\left(d^3 - h^3\right)\sin^3\left(\theta/2\right)}{3\left(d^2 - h^2\right)\left(2\pi - \theta + \sin\theta\right)} \tag{A.12}$$

Then, the nominal moments in the steel cross section can be summed as:

$$C_s Y_{cs} + T_s Y_{ts} = F_y Z_{s\theta} \tag{A.13}$$

From Equation A.13, the plastic modulus of the steel cross-section for any angle theta is given by:

$$\begin{aligned} Z_{s\theta} &= \frac{\theta\left(d^3 - h^3\right)\sin^3\left(\theta/2\right)}{12\left(\theta - \sin\theta\right)} \\ &\quad + \frac{\left(2\pi - \theta\right)\left(d^3 - h^3\right)\sin^3\left(\theta/2\right)}{12\left(2\pi - \theta + \sin\theta\right)} \end{aligned} \tag{A.14}$$

In the denominator of the second term of Equation A.14, the sin(θ) term may be taken as its trigonometric equivalent, –sin(2π – θ). With all like terms based upon the same angle, 2π – θ, Equation A.14 can be restated as:

$$\begin{aligned} Z_{s\theta} &= \frac{\left(d^3 - h^3\right)\sin^3\left(\theta/2\right)}{12} \\ &\quad \times \left[\frac{\theta}{\left(\theta - \sin\theta\right)} + \frac{\left(2\pi - \theta\right)}{\left(2\pi - \theta\right) - \sin\left(2\pi - \theta\right)}\right] \end{aligned} \tag{A.15}$$

Equation A.15 is the one shown in Table 5 (Point B) in the original paper to get the plastic section modulus (Z_s) of a circular HSS.